



HAL
open science

Mapping the Most Energetic Cosmic Rays

A.M. Hillas

► **To cite this version:**

A.M. Hillas. Mapping the Most Energetic Cosmic Rays. *Astroparticle Physics*, 2009, 32 (3-4), pp.160.
10.1016/j.astropartphys.2009.07.005 . hal-00498976

HAL Id: hal-00498976

<https://hal.science/hal-00498976>

Submitted on 9 Jul 2010

HAL is a multi-disciplinary open access archive for the deposit and dissemination of scientific research documents, whether they are published or not. The documents may come from teaching and research institutions in France or abroad, or from public or private research centers.

L'archive ouverte pluridisciplinaire **HAL**, est destinée au dépôt et à la diffusion de documents scientifiques de niveau recherche, publiés ou non, émanant des établissements d'enseignement et de recherche français ou étrangers, des laboratoires publics ou privés.

Accepted Manuscript

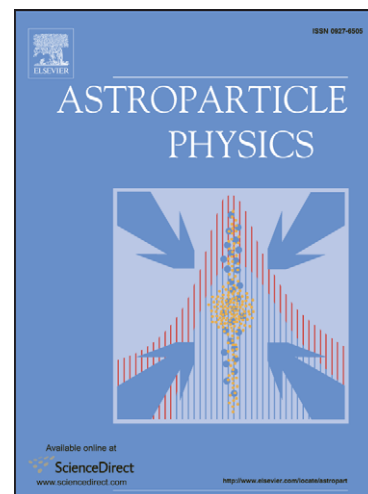
Mapping the Most Energetic Cosmic Rays

A.M. Hillas

PII: S0927-6505(09)00109-1
DOI: [10.1016/j.astropartphys.2009.07.005](https://doi.org/10.1016/j.astropartphys.2009.07.005)
Reference: ASTPHY 1425

To appear in: *Astroparticle Physics*

Received Date: 19 May 2009
Revised Date: 11 July 2009
Accepted Date: 16 July 2009



Please cite this article as: A.M. Hillas, Mapping the Most Energetic Cosmic Rays, *Astroparticle Physics* (2009), doi: [10.1016/j.astropartphys.2009.07.005](https://doi.org/10.1016/j.astropartphys.2009.07.005)

This is a PDF file of an unedited manuscript that has been accepted for publication. As a service to our customers we are providing this early version of the manuscript. The manuscript will undergo copyediting, typesetting, and review of the resulting proof before it is published in its final form. Please note that during the production process errors may be discovered which could affect the content, and all legal disclaimers that apply to the journal pertain.

Mapping the Most Energetic Cosmic Rays

A.M. Hillas

School of Physics and Astronomy, University of Leeds, Leeds LS2 9JT, UK

Abstract

The Pierre Auger Collaboration has shown that the cosmic rays detected to August 2007, with estimated energies above 57 EeV, were mostly very close to the direction of a catalogued AGN within ~ 75 Mpc. The closeness of the sources to us, and their association with the locality of moderate Seyfert galaxies rather than the most striking radio galaxies, were surprising, leading some authors to question the reality of the apparent associations. Here, three further techniques for examining the correlation of cosmic ray arrival directions with directions of AGNs are introduced to confirm and extend this correlation. These include the uniform-exposure polar plot to examine large-scale associations, and a sensitive “right ascension resonance” test to show the rapidity of the decoherence when the two patterns are displaced. The latter test avoids the choice of a correlation window radius, which makes it possible to see an AGN correlation in other data at a lower energy, and to seek it in HiRes data. On the basis of the closeness of correspondence of the cosmic ray and AGN maps, and the equally significant correspondence with directions of extended radio galaxies listed by Nagar and Matulich but not used in the Auger group’s investigation, it is argued that the association with these two sets of objects is by no means accidental, although the efficacy of the 57 EeV “cut” in selecting this revelatory sample may have been accidental.

The arrival directions of these cosmic rays (average energy 75 EeV) can be well described if most of the sources are in or around rather typical Seyfert galaxies, in clusters typically at ~ 50 Mpc, with the cosmic rays being scattered by $3\text{--}4^\circ$ on their way to us. Because of close clustering of AGNs, it cannot usually be ascertained which object within 2–3 Mpc is the actual source, but more than a third of the cosmic rays appear to come from FRI or similar radio galaxies in the clusters. It thus seems likely that these and also weaker jet-forming Seyfert galaxies are indeed causing acceleration to 10^{20} eV. Neither the brightest (nearby) radio galaxies nor the Virgo cluster dominate the cosmic-ray sky as had been expected, and Cen A is probably one of the currently inactive 10^{20} eV accelerators, as much more distant FRI galaxies play such a large role. The deflections cannot be much more than $3\text{--}4^\circ$ without destroying the coherence. Intergalactic magnetic fields ~ 1 nG could be responsible, but in one part of the sky a displaced “resonance” suggests a possible 4° deflection by the B_z component of our local Galactic magnetic field. A source region limited to <120 Mpc for the Auger cosmic rays is supported. This is compatible with a GZK survival horizon but only if (a) the sudden fall in the energy spectrum is not simply a GZK effect but essentially reflects the energy cut-off in the accelerators, and (b) the Auger energies are underestimated by $\sim 25\%$.

Key words: Cosmic ray origin, AGNs, Equi-exposure skymap

1 **1. Introduction to the new observations of arrival directions of the most energetic cosmic** 2 **rays**

3 In 2007 the Pierre Auger Collaboration [1] published the directions of arrival of 27 cosmic-
4 ray particles which they estimated to have energies above 5.7×10^{19} eV (57 EeV), and near
5 most of these directions (within 3.2°) there was an active galactic nucleus (AGN) listed in the
6 12th Véron-Cetty Véron catalogue (abbreviated below as VCV) [2] within a distance of about
7 75 Mpc of Earth (if $H_o = 72 \text{ km s}^{-1} \text{ Mpc}^{-1}$, as assumed below). The probability of such a close
8 association appeared to be very small if the cosmic rays arrived from near-random directions as
9 only 21% of cosmic rays would be expected to match so closely in this case. By contrast, many
10 air shower experiments had previously sought evidence for the sources of cosmic rays above
11 10^{17} eV, but had failed to find any convincing departures from isotropy, supporting the belief that
12 deflections of the particles in irregular magnetic fields had scrambled their directions of motion.
13 Above about 60-80 EeV, though (depending on the maximum energy of particles leaving the
14 sources), few protons or light nuclei would reach us from beyond very few hundred Mpc because
15 of energy losses in the cosmic microwave background radiation (the GZK effect in the case of
16 protons, or photodissociation of nuclei), and so the particles from far off, that would have been
17 highly deflected en route, should be absent. The Auger experiment in Argentina is unique in its
18 huge collecting aperture, its very uniform sensitivity to cosmic rays above 10^{19} eV (within 60°
19 of the zenith), well-measured energies in this context, and, apparently, an inspired unexpected
20 choice of the VCV catalogue to check for significant patterns in the arrival directions. The data
21 set will be greatly expanded in the next few years, but it already shows that, firstly, the most
22 spectacular double-lobe radio galaxies that dominate the radio sky are not the principal suppliers
23 of these extreme cosmic rays, secondly, the expected beacon of the local skies, the Virgo cluster,
24 is also relatively unimportant, and in fact most of these extreme cosmic rays appear to originate
25 in less remarkable Seyfert galaxies or else in sources that cluster in their vicinities (say 2-3 Mpc).
26 Looking outside the VCV catalogue of optically-detected AGNs used in the Auger report, it is
27 found additionally that a considerable minority of these cosmic rays correlate about as closely,
28 and perhaps even more significantly, with extended radio galaxies within the same distance range,
29 although somewhat further away than those which dominate the radio sky: a set of sources
30 brought to our attention by Nagar and Matulich [3]. Very fortunately, it seems that, at these
31 energies, deflections of the particles over 100 Mpc are not more than a few degrees. However,
32 it will be proposed that this description applies only to the proton component of cosmic rays,
33 whereas there is evidence that above 40 EeV most particles are highly charged; so a detector's
34 bias in favour of protons may strongly influence the pattern that it sees.

35 It is a novel feature for charged-particle astronomy to reveal a rich pattern of point sources,
36 and these surprises have led to challenges. It is the first main object of this paper to provide
37 further methods of analysis that greatly strengthen the evidence that these details of the arrival
38 patterns are real, and then to examine the most probable implications regarding the origin, nature
39 and energies of the particles, that can be straightforwardly tested with more data.

40 The unexpectedness of these reported correlations led commentators to express doubts of
41 many kinds. First, regarding the methodology, it has been suspected that the apparent statisti-
42 cal significance of the result has been artificially generated by the use of the first half of the
43 Auger observational data set to vary the selection "cuts" in energy threshold, maximum redshift
44 of catalogued AGNs to be used in the correlation, and the correlation window size — all cho-
45 sen to maximize the significance of the departure from isotropy in this first subset. However,
46 as explained below, these values proved to be very nearly optimum for the whole dataset. Sev-

47 eral early discussions of the arrival directions have put aside the apparent close correlation with
48 weak AGNs, and considered large magnetic displacements from the directions of expected strong
49 sources [4, 5, 6]. The use of the VCV catalogue based on optical appearance of galaxies, rather
50 than one with more emphasis on high jet luminosity indicated by strong radio or X-ray emission,
51 has been questioned [7, 8]. Different proportions of AGNs will be included in the catalogue in
52 different regions of space. A deduction that most of the sources are less than 100 Mpc away
53 has been remarked on as strange [9]. The northern-hemisphere HiRes experiment found no as-
54 sociation of the most energetic cosmic rays with AGNs [10]. The very weak level of activity of
55 some of the AGNs picked out in the study has been remarked on as making their identification as
56 cosmic-ray sources implausible. (It should be pointed out that the Auger authors did not claim to
57 discriminate between the AGNs and other objects that reside in the same localities as the AGNs.
58 Their published study was intended to demonstrate anisotropy rather than to explain it at this
59 stage.)

60 Whilst the aim of the research is to understand how particles are accelerated to these extreme
61 energies [4, 5, 9], the emphasis in this paper is on extracting as clearly as possible the simplest
62 pointers to sources that are present in the cosmic-ray directional data, largely avoiding scrutiny of
63 particular accelerators. When three times the presently published data set is available, it should
64 be possible to pay attention to individual sources. So it is the purpose in this paper to tackle
65 many of these doubts, and to show that the evidence can be extended. The clumpy pattern on the
66 sky of these AGNs can be demonstrated by a simple extension of the Auger “window” counts,
67 and these clumpy distributions of cosmic rays and AGNs on the sky can be better visualised and
68 quantified by an alternative form of mapping, using a uniform-exposure polar plot. A simple
69 model of apparent origins of cosmic rays scattered around VCV AGN locations describes also
70 the overall pattern of the cosmic rays. (The clumping also implies that not all AGNs near the
71 cosmic-ray line of sight are necessarily the relevant sources, so several objects can have been
72 misidentified as sources.) A “right ascension resonance” test is introduced as a striking and
73 sensitive demonstration of the association with AGN localities, using which such associations
74 can later be sought using a different list of potential sources, in data of other experiments, and
75 potentially at other energies, and a hint of magnetic deflection appears.

76 The work is laid out as follows. The direct evidence of the density and clustering of AGNs
77 near cosmic-ray directions is examined in section 2, showing that the particles do not come
78 precisely from the AGNs, but are distributed within $\sim 3-4^\circ$. In section 3, the use of the uniform-
79 exposure polar plot is introduced, to show where these clusters are on the sky, and demonstrating
80 first the anisotropy of the cosmic-ray distribution without regard to AGNs, and then that its large-
81 scale features do match those of the AGNs in the VCV catalogue (which has a “useful” distance
82 bias), apart from a possible anomaly in the direction of the Virgo cluster, which will be re-visited
83 later. Section 4 introduces a “right ascension resonance” as an alternative to the Auger method
84 of detecting a correlation of cosmic ray directions with AGNs, but not requiring the choice of a
85 particular “window radius” for counting nearby AGNs, and avoiding the large statistical penalty
86 which the choice of this radius involves. Using this, an AGN association can be sought in the
87 results of two experiments viewing the northern hemisphere. In section 5, the correlation of
88 cosmic rays with an alternative set of AGNs, “extended radio galaxies” [3], will be considered.
89 In section 6 the resonance technique is used to seek evidence of magnetic deflections where
90 particles arrive after following a long path just above the disc of our galaxy. Section 7 explores
91 the extent in redshift of the AGN correlation, finding rough agreement with the Auger group’s
92 conclusion that most of the particles reaching us at these energies have travelled less than 100
93 Mpc. In section 8, it is argued that this implies an underestimation of particle energies, and also

94 implies that the reported steep fall in the cosmic-ray spectrum is not simply a “GZK spectrum
 95 cutoff”, but largely a downturn of the energy spectrum of the accelerators, which imposes a
 96 “GZK distance horizon”; but the details are sensitive to probable energy measurement errors.
 97 Some principal conclusions are summarized in section 9.

98 Appendix A introduces some relevant shortcomings of the VCV catalogue of optically-
 99 detected AGNs, which limit the range of source distance for which this catalogue can be used.
 100 Figure 13 in the appendix shows the number of objects visible from the southern hemisphere that
 101 are listed per Mpc of distance and in different ranges of absolute magnitude, which indicates that
 102 the completeness of the catalogue for fainter objects (some of which may nevertheless be particle
 103 accelerators) is continually decreasing with increasing distance, and that beyond about 75 Mpc
 104 the gaps may be serious, so that it will be more difficult to use the VCV catalogue to explore
 105 further into space (as remarked in [1]). If the number of listed AGNs per square degree had been
 106 much greater, however, the probability of accidental associations within 3.2° with any arbitrary
 107 direction would have been large, nullifying the signal. A sparser but uniform catalogue would
 108 be better for such an exploration, and it will be seen that a catalogue of FRI radio galaxies may
 109 serve well here. Indeed following up the suggestion of Nagar and Matulich [3], the correlation
 110 with such objects already adds substantially to the significance of these associations.

111 2. Clustering of the AGNs: the cosmic ray source is often not the closest AGN

112 The evidence that these most energetic cosmic rays originate in the locality of AGNs was that,
 113 excluding 6 cosmic rays arriving within 12° of the galactic plane, where most AGNs would be
 114 obscured by dust, and where cosmic rays might be more strongly deflected by galactic magnetic
 115 fields, only 2 of the remaining 21 cosmic ray directions did not have an AGN (redshift < 0.018)
 116 within an angular radius of 3.2° , whereas if one places such 3.2° windows at arbitrary positions on
 117 the sky, governed only by the total exposure of the detector array to each region (but avoiding the
 118 vicinity of the galactic plane), one finds only 24% of them contain AGNs.¹ (The average *number*
 119 of AGNs per window is 0.36.) This striking aspect of the figures goes somewhat beyond what
 120 was emphasised in the Auger paper, which properly took a more cautious approach in the first
 121 instance, not excluding use of the galactic obscuration zone, which is only crudely represented
 122 by a simple 24° -degree-wide belt. As the authors use two slightly different sets of data cuts,
 123 these will be mentioned here to avoid possible confusion later. When about half of the published
 124 cosmic rays had been recorded (14 of the 27 events), it was found that the departure from isotropy
 125 had reached a predetermined high level of significance if one took a cosmic-ray energy threshold
 126 of 56 EeV, and counted VCV AGNs with redshifts ≤ 0.018 , within a window of 3.1° radius
 127 around each cosmic-ray direction. These same cuts were then used for the cosmic rays detected
 128 later, and this enhanced set of cosmic rays fully confirmed that the arrival directions were not
 129 isotropic. Using the full data set, the cuts were re-optimized to maximize the significance of
 130 anisotropy, and the resulting values, only slightly different from the original set, were 57 EeV
 131 for the threshold, redshifts < 0.018 (equivalent to ≤ 0.017 in the VCV catalogue), and window
 132 radius 3.2° degrees. The small change in redshift range would not affect the counts discussed
 133 below, though the increase in window radius adds two associations in the first half of the run,
 134 changing a “hit rate” 8/10 to 10/10 (with obscuration zone excluded), so the window radius is a
 135 very sensitive parameter.

¹Note that the proportion 21% quoted by the Auger authors applies if the galactic obscuration zone is not excluded from the counts.

136 Though the statistics seem, and are, significant, the precise figures are clearly sensitive to
 137 the choice of cuts, and especially the window radius, so it seems desirable to check on the bias
 138 introduced in such a choice by using a less capricious measure of closeness of the cosmic-ray and
 139 AGN directions. There is no physical reason for expecting 3.2° to be appropriate: this value may
 140 serve mainly to minimize the chance of random unassociated AGNs being counted in a crowded
 141 sky. The next paragraph will, incidentally, supply support for the supposition that the galactic
 142 belt should be excluded.

143 The low average density of 0.36 AGNs (in this catalogue and in this redshift range) per
 144 3.2° window might be thought to indicate that when an AGN is seen in the window it must
 145 probably be the source of the cosmic ray particle, but this is not so, firstly because the AGNs
 146 are strongly clustered. The average number of AGNs per window drawn around the 21 selected
 147 cosmic rays (“window 1”, below) is 1.1, but the average numbers in the 3 surrounding annuli
 148 $3.2^\circ - 4.53^\circ$, $4.53^\circ - 5.54^\circ$ and $5.54^\circ - 6.40^\circ$ (“windows 2 to 4”, below), all of equal solid angle,
 149 are given in line (A) of the table 1.

window number	1	2	3	4
(A) $\langle N_{\text{AGN}} \rangle$ in windows around CR	1.1	1.1	1.0	0.7
(B) $\langle N_{\text{otherAGN}} \rangle$ around selected AGN	1.2	0.9	0.9	0.8

Table 1: Numbers of AGNs in concentric annuli.

150 Line (A) shows that there is typically a high local density of AGNs which extends for several
 151 more degrees. To find the typical density of AGNs in any region inhabited by AGNs, one can
 152 draw windows and surrounding annuli around any AGN, and line (B) of the table shows the
 153 average number of other AGNs found in these windows (the average being weighted by the array
 154 exposure at that declination, and avoiding the zone of low galactic latitude). The AGN densities
 155 around cosmic ray directions are little different: clearly an “other AGN”, unrelated to any that
 156 might be the cosmic ray source, is very likely to be found in the central window; so the AGN
 157 seen in the standard 3.2° window used by Auger may often be a neighbour unrelated to the
 158 cosmic ray. Indeed, if the cosmic rays always pointed back very close to a source AGN (always
 159 well within 3.2°), one would expect the numbers in line (A) to be like those in line (B) except
 160 for an additional 1 in the central window (because we are now counting the “central” AGN in
 161 addition to the “other” AGNs that were counted in line (B)), and the count in windows 1 and 2
 162 of line (A) would be expected to differ by about 1.0, which they do not. A precaution is needed
 163 before carrying this arithmetic further, because the counts in the central window (window 1 in
 164 the above table) will be biased, perhaps especially in the first half of the data sample, which was
 165 used to optimize the data cuts. (In this first half of the data, the average number of AGNs per
 166 window is 1.1 but there are no zeros — a quite un-poissonian distribution!) Using the second
 167 half of the data, with only 11 showers outside the zone of low galactic latitude, the numbers
 168 of AGNs seen, this time in successive ranges of 2.5° from the cosmic ray direction, have been
 169 counted, and are shown in table 2 in the line “OBS”, their numbers expressed as density per
 170 9.80×10^{-3} steradian, this being the area of the standard 3.2° window. The excess number of
 171 counts at the closest distances is sensitive to how far cosmic rays are spread around a “source”
 172 AGN (either by magnetic scattering or by the size of a cloud of supposed accelerators such
 173 as magnetars or hypernovae). One can simulate the numbers of AGNs that would be found at
 174 different distances from a cosmic-ray direction if they are typically spread with r.m.s. distance
 175 3.2° , 4° or 5° , for example, around AGNs chosen randomly from the catalogue, but then accepted

176 with a probability matching the observational exposure to that declination. (One can only take a
 177 very simple approach in such a small sample, and the question of whether an AGN closer to us
 178 should have been given a higher weight will be taken up later.) The results are shown in table
 179 2 as “SIM 3.2° spread”, “SIM 4.0°” and “SIM 5.0°”. Of several examples calculated, the r.m.s.
 180 spread of 4° gave the nearest match to the observations, though the scanty statistics do not offer
 181 much precision (though a spread in accordance with this will be estimated in other ways later).

angular distance (°)	0	2.5	5	7.5	10	12.5	15
OBS	1.49	0.89	0.78	0.60	0.53	0.46	
SIM 3.2° spread	1.75	1.13	0.79	0.65	0.58	0.54	
SIM 4.0° spread	1.48	1.11	0.82	0.66	0.58	0.54	
SIM 5.0° spread	1.24	1.05	0.83	0.68	0.60	0.54	

Table 2: Surface density of AGNs near cosmic ray directions.

182 The observations thus suggest that cosmic-ray arrival directions have an r.m.s. spread of
 183 about 4° around typical AGNs, although this cannot be a universal constant as the AGNs will
 184 of course be at different distances. The AGN density remains considerably above the average
 185 density of 0.36 for $\sim 10^\circ$, indicating the typical extent of AGN clusters.

186 Thus the cosmic rays may suffer magnetic scattering of 4° while travelling to the observer
 187 from an AGN source. Since this is somewhat greater than the 3.2° radius of the Auger selection
 188 window, one should not place too much emphasis on the type of AGN found closest to the
 189 cosmic ray or even in the window. The true source may well lie outside the window; and *a prime*
 190 *reason why some AGN is almost always seen in the window is because they are so crowded in*
 191 *the region around the source.* The appearance of particularly feeble objects in the list need not
 192 cause surprise. Thus Zaw, Farrar and Greene [11] noted that whilst most objects picked out
 193 by these windows were AGNs with bolometric luminosities above $0.5 \times 10^{43} \text{ erg s}^{-1}$, in two
 194 other cases the neighbouring objects had been misidentified as AGNs. It is found that a very
 195 strong association with cosmic rays still persists if only radio-detected AGNs are retained in the
 196 catalogue (about 75% of all those listed). One probably has a mixture of galaxy types close by
 197 in typical clusters, and one can deduce only that the sources lie in or near AGNs of a type that is
 198 very common in such clusters — say comprising 1/3 or more of the population. But the evidence
 199 so far does not prove that AGNs are sources. Since unusual activity in galactic nuclei, and growth
 200 of supermassive black holes, is believed to arise from collisions between galaxies in clusters, it is
 201 also possible that the AGNs are not the sources but are serving as markers of regions where other
 202 types of activity related to star formation are also concentrated. The role of AGNs as markers
 203 of concentrations of general galactic activity has been taken up by Ghisellini et al. [12], who
 204 showed that clusters of ordinary galaxies did indeed correlate with Auger cosmic ray directions.

205 Much of the following discussion will avoid the choice of a “window” of a particular radius,
 206 but before moving on it is worth mentioning that, of the windows around the 6 cosmic rays in
 207 the galactic exclusion zone, somewhat crudely set at a uniform belt within 12° of the galactic
 208 plane, only 1 contains a VCV AGN and the first two surrounding annuli contain only 1 AGN in
 209 all (12 annuli). These do appear to be regions almost devoid of visible AGNs, supporting their
 210 designation as obscured regions where we do not know the positions of AGNs, as this catalogue
 211 is based on optical surveys, so tests of association cannot be performed (though the bright radio
 212 source Cen B does shine through the dust and coincides with a cosmic ray).

213 Where are these AGN clusters? The large scale features of the cosmic ray directions and

214 associated AGNs will be examined in the next section.

215 3. Mapping the sky on a uniform-exposure polar plot

216 The Aitoff sky projection that is commonly used to show how cosmic-ray arrival directions
 217 relate to large-scale astronomical features can illustrate the relationship between clear-cut struc-
 218 tures, but is less suited to these irregular and clumpy patterns. Not only does the varying ef-
 219 ficiency of detecting cosmic rays in different parts of the diagram disguise real variations in
 220 intensity, but adjacent regions are cut apart, and important great circles such as the galactic plane
 221 twist sharply, making it hard to see whether the cosmic ray patterns relate to these planes. The
 222 pattern of cosmic ray arrival directions is revealed much better in a uniform-exposure polar plot,
 223 described below, if one is content to display one hemisphere, or slightly more, rather than the
 224 whole sky.

225 Although I first used this plot in the 1970s in correspondence about the Yakutsk observations,
 226 it was not fruitful then, as no patterns emerged, and I regret not having published it, although it
 227 has been used a few times in publications by colleagues (e.g. [13]). Only now, with many
 228 particles detectable above the GZK barrier, is a study of tens, rather than thousands of arrival
 229 directions of great interest again.

230 Figure 1 shows such a plot, for the 27 Auger cosmic rays. The plots are always centred on
 231 a pole — the south celestial pole in this case. If δ is the declination of a point in the sky, and
 232 p its polar distance, ($p = 90^\circ - \delta$ for a north polar plot or $p = 90^\circ + \delta$ for a southern plot),
 233 the radial coordinate, R , in the plot, representing polar distance, is non-linear, being adjusted
 234 according to the total exposure of the observatory to each band of declination, so that the area
 235 of any band of p is proportional to the number of particles that would be detected in that band
 236 if the particles arrived at the earth isotropically. Particles detected from an isotropic flux would
 237 then yield a plot with a uniform density of points per unit area, apart from the usual accidental
 238 statistical fluctuations.

If, for an isotropic flux, one detects $n_p(p)$ particles at polar distances less than p , out of a total
 of n detected particles,

$$R = \sqrt{(n_p/n)} \quad (1)$$

239 (The diagram has unit radius.) The azimuthal angle $\phi = \alpha$, the right ascension. A comment is
 240 appropriate here for the armchair astronomer. With this choice of α (increasing anticlockwise),
 241 this diagram looks very much like a true spherical sky globe seen from within in the case of the
 242 southern sky (and so represents the sky much as it really looks): but a northern hemisphere plot
 243 would look much like a sky globe viewed from the outside (giving a left-to-right mirror image
 244 of the constellations). In the north, this physicist's convention for plotting right ascension can
 245 be disconcerting to those astronomers who actually look at the sky, but will have the advantage
 246 of allowing the viewer to follow features such as the Virgo supercluster continuously from one
 247 hemisphere to the other.

248 If the observatory can record cosmic rays arriving at any point on a well-defined ground area,
 249 A , independent of their zenith angle of arrival, θ , out to a maximum zenith angle θ_{max} — as is
 250 the case for the Pierre Auger Observatory at energies above 10^{19} eV, with $\theta_{max} = 60^\circ$ — the
 251 detection efficiency at each declination or polar distance is well defined and the radial scale $R(p)$
 252 in equation 1 can be derived from first principles. For the Auger case, with $\theta_{max} = 60^\circ$ and
 253 latitude -35.2° , the radius R is tabulated in appendix B, table 4; alternatively an approximate
 254 formula can be used, such as equation (5) in the appendix, which has a maximum error of 0.006.

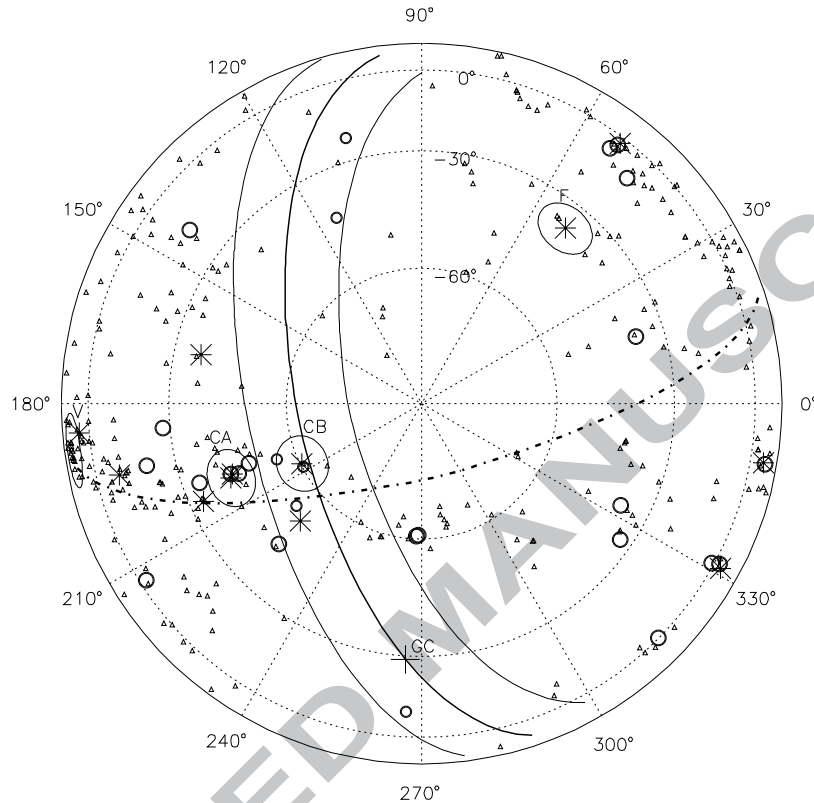


Figure 1: The 27 arrival directions of particles above 5.7×10^{19} eV, published by Abraham et al. [1] on a uniform-exposure polar plot. The 6 particles within 12° of the galactic plane are shown as smaller circles. NB: near R.A. 268° , dec. -61° there are two cosmic rays extremely close together. The galactic plane and circles of galactic latitude $\pm 12^\circ$ are shown as full lines (GC marking the galactic centre) and the supergalactic plane as a dot-dash curve. Declination circles at 30° intervals, and radial right ascension lines, are shown dotted. Circles of 6° radius drawn around some of the strongest radio galaxies – V, Virgo A (M87), CA, Cen A, CB, Cen B and F, Fornax A – illustrate the compression of the radial scale towards the edge. (A 6° circle represents the angular distance from a source within which (at ~ 40 Mpc) most of these cosmic rays arrive according to the analyses discussed here.) Virgo A is at the centre of the Virgo cluster of galaxies. Small triangles mark the positions of 280 VCV AGNs S of declination $+18^\circ$, having redshifts < 0.018 . Eight-armed crosses (stars) mark the extended radio galaxies listed in [3].

255 Polar angles appreciably beyond 114° are unobservable — and off the diagram. In other cases,
 256 one would generally use data on the relative numbers n_p/n of detected particles in some well-
 257 defined lower energy band, close enough to 57 EeV (or whatever) for the detecting conditions to
 258 be virtually the same, but low enough for the particles to be approximately isotropic and much
 259 more numerous. Substitution of these numbers in equation 1 gives the radial scale $R(p)$ for the
 260 plot.

261 Even without considering a connection with AGNs, the 27 Auger showers shown in figure 1
 262 appear to be distributed non-randomly, but the eye and brain will usually imagine an interesting
 263 relationship in a pattern of dots (“canals on Mars”). To characterize the clumpiness of the pattern

264 of points, the cumulative distribution of the 351 inter-point distances Δ as measured on the plot
 265 is shown in figure 2, and the average sky separation in degrees corresponding to the various
 266 separations Δ on the uniform-exposure plot are shown along the bottom of the graph.

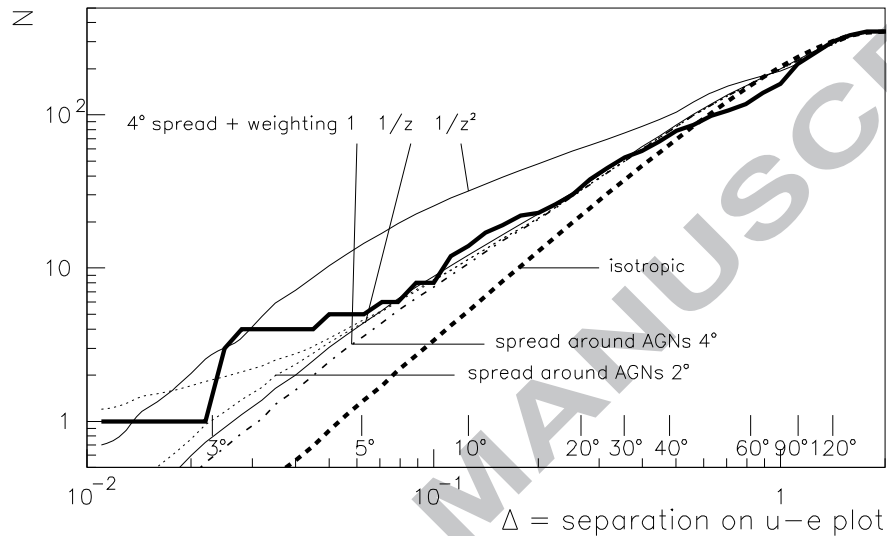


Figure 2: Cumulative number N of inter-point distances Δ on uniform-exposure plot in figure 1 for the 27 Auger cosmic-ray directions. The average separations in degrees on the sky, to which these plot-separations Δ refer, are shown just above the horizontal axis. Thick line: the observations (fig 1). Thick dashed line (“isotropic”), shows the average $N(\Delta)$ for many sets of 27 points placed randomly on the plot, simulating cosmic rays approaching the earth isotropically. Dot-dash line: average $N(\Delta)$ for many sets of 27 directions of AGNs picked from the VCV catalogue (redshifts $z < 0.018$) and given a 4° rms scatter (with refinements described in the text). Changing the scatter to 2° or 0.5° produces the variants shown by dotted lines. If a distance weighting is applied when picking AGNs, a $1/z^2$ weighting (appropriate if catalogue unbiased) moves the (4°) curve to the upper thin full line; the preferred $1/z$ weighting (see text) gives the full-line curve little different from the unweighted (dot-dash) version.

267 When compared with the inter-point distances found in a large number of sets of 27 points
 268 placed randomly on the circular plot, the cosmic rays show a large excess of separations at all
 269 angles below 30° , clearly non-random, as fewer than 1 in 400 of the random sets match the high
 270 number of inter-point distances in the range $10^\circ - 14^\circ$, related to the size of clumps. The cosmic
 271 rays are thus clumpy quite apart from what AGNs tell us. (An analogous test for randomness was
 272 reported in the Auger paper [1], based on inter-event distances on the sky, rather than on an equal-
 273 exposure plot.) To test how well the AGN distribution as a whole accounts for this large-scale
 274 pattern, one can construct simulated sets of 27 cosmic ray directions by picking AGNs randomly
 275 from the catalogue, choosing a “cosmic ray direction” by applying a Gaussian displacement
 276 of rms angle 4° (Gaussian displacements of $4^\circ/\sqrt{2}$ in two perpendicular directions), and then
 277 accepting the direction with a probability given by the Auger array detection efficiency at that
 278 declination (table 4). There is a complication, as 20% of the sky is effectively occupied by
 279 the galactic zone in which many AGNs are hidden, so most of the cosmic rays within 12° of
 280 the galactic plane are not reproduced in such a simulation. It seems, in fact, not to change the
 281 inter-point distribution greatly, but to check this, a population of simulated cosmic rays has been

282 generated by adding “infilled” fake AGNs in the galactic exclusion zone, by a process of copying
 283 random AGNs of rather similar supergalactic latitude and shifting them in supergalactic longitude
 284 into this zone. The distribution of inter-point distances for these simulated cosmic ray directions
 285 is shown by the dot-dashed line in Figure 2, and the effect of reducing the r.m.s. scatter about the
 286 AGN directions to 2° or 0.5° is shown by two dotted lines. They fit the observed distributions
 287 rather well except for a strange deficit, in real cosmic rays, of separations near 50° – low gradient
 288 of distribution — with an excess (steeper gradient) near 80° (separations near 0.7 and 1.0 on the
 289 plot). There is also one exceptional small separation; and three more around 3° may lie outside
 290 the average distribution, but some of these could occur quite naturally. One of the latter is aligned
 291 with the very close AGN Cen A (3.4 Mpc), so if Cen A *is* the source, deflections could possibly
 292 be reduced in this case. Also, if these cosmic ray “deflections” represent magnetic scattering
 293 in a patchy magnetic field, the angle between a pair of arriving particles of similar energy from
 294 one source can be appreciably less than the typical overall deflection, so a simple model of
 295 independent deflections will underestimate the frequency of arrival of close pairs. (Apart from
 296 one unusually energetic event, the rms energy spread of the Auger particles is only 15%.) The
 297 overall pattern of cosmic rays on the sky thus supports the supposition of their emission from the
 298 localities of AGNs.

299 But this process of selecting randomly the AGNs to serve as source locations ignores the $1/z^2$
 300 geometrical attenuation of cosmic ray flux that should occur when deflections are small, favouring
 301 the AGNs closest to us, and also ignores an opposite correction for the incompleteness of the
 302 catalogue at greater distances. Regarding the latter point, in figure 13, the distance distribution of
 303 the brightest objects, which would suffer least from a flux detection threshold, varies as $dn/dz \propto z$
 304 at low z , as would happen in the case of matter distributed uniformly in a thin slab, though the
 305 angular spread of AGNs seen in figure 1 indicates that they spread much more widely than a slab
 306 configuration, so the real dn/dz distribution is probably tending towards a more isotropic z^2 vari-
 307 ation at larger z . The overall trend of all catalogued AGNs in figure 13 is roughly $dn/dz \propto z^{0.3}$,
 308 so the numbers of catalogued AGNs may have to be multiplied by a factor in the range $z^{0.7}$ to
 309 $z^{1.7}$ to correct their apparent space density. When combined with the cosmic ray geometrical
 310 flux attenuation factor $1/z^2$ this suggests that the most reasonable distance-weighting factor for
 311 selecting “source AGNs” would be in the range $z^{-1.3}$ to $z^{-0.3}$. A distance-weighting factor $1/z$
 312 is a reasonable compromise for the present (stopping the variation at $z < 0.001$ to avoid infinities),
 313 and the use of this factor made a slight improvement to the modelled curve in figure 2, shown
 314 by a full line slightly above the previous “model” curve (dot-dash). If the catalogue had been
 315 supposed equally complete at all distances, and the factor $1/z^2$ thus applied (down to $z = 0.001$),
 316 the very discordant higher curve is obtained, as a few extremely close sources dominate, very
 317 much at variance with the observations.

318 The Auger paper showed that where there are cosmic rays of such extreme energies there are
 319 AGNs nearby. Are there cosmic rays wherever there are AGNs (within 75 Mpc)? The overall
 320 clumpiness of the cosmic ray distribution has been shown to be consistent with this; different
 321 source regions are examined next.

322 Figure 3 divides the equal-exposure plot into 50 segments of equal area, a coarse resolution
 323 which seems appropriate for this situation. (Five annuli, of equal radial thickness, are subdivided
 324 into 2, 6, 10, 14 and 18 equal segments in right ascension.) To compare the distribution of
 325 detected cosmic rays with that of VCV AGNs (with redshifts < 0.018) as potential sources,
 326 in figure 3 each AGN was in version (a) simply given a weight proportional to the detection
 327 efficiency of cosmic rays from that direction, and the (rounded) total weighted number of VCV
 328 AGNs is printed in each segment, or in plot (b), a distance-dependent factor proportional to $1/z$

329 was also included in the weight, as suggested above. In both version (a) and (b), the weights
 330 were scaled to give 1 on average within a radius of 0.75 in the diagram. In the simple version (a)
 331 the weight was then 1.61 in the centre.

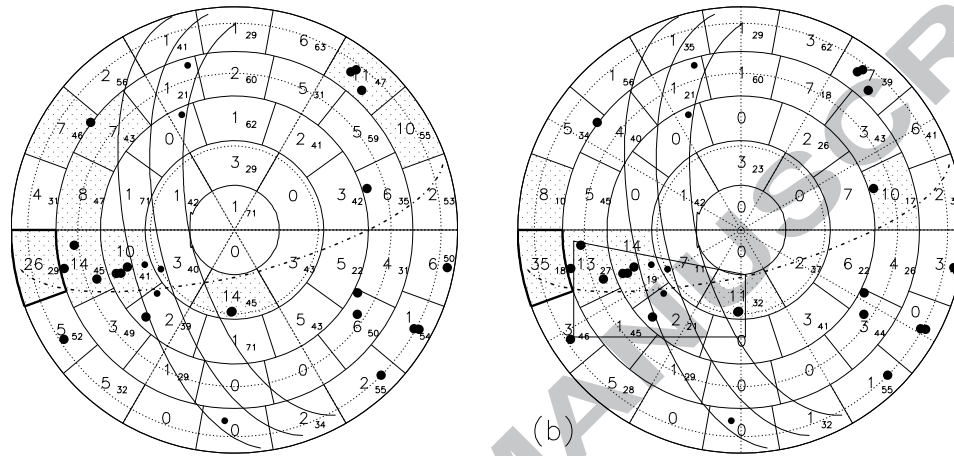


Figure 3: The uniform-exposure plot divided into 50 segments of equal area. (a) The larger numerals give the (rounded) number of VCV AGNs (at a redshift $z < 0.018$) in each segment, weighted by a relative array exposure factor (made to average 1 for radii < 0.75 , going to zero at the outer edge). Smaller numbers: weighted average distance of these AGNs, in Mpc. The 9 segments with weighted AGN count > 6 are shaded. (b) The same, but weight given to each AGN includes an additional factor $\propto 1/z$ (still normalized to 1): see text. Here the 6 segments with > 7 (weighted) AGNs are shaded.

332 In order to compare cosmic ray and AGN patterns, only the 21 cosmic rays outside the $\pm 12^\circ$
 333 galactic exclusion zone will be used: the cosmic rays clearly favour the segments containing
 334 many VCV AGNs. The numbers in (a) count AGNs when the only weighting is the exposure
 335 efficiency (version a), and in the 41 of these 50 segments that contain only 0 to 6 (weighted)
 336 AGNs, there are 101 of the 208 AGNs and 9 cosmic rays: the ratio CR/AGN is 0.09. In the whole
 337 diagram the ratio $CR/AGN = 21/208 = 0.10$. So even where AGNs are sparse, the proportion
 338 of cosmic rays is not lower than in the denser regions, suggesting in this small available sample
 339 that one does not need an exceptionally massive or rare AGN, such as is found at the centre of
 340 a large cluster, to supply cosmic rays. But the heavily-outlined Virgo segment has 26 weighted
 341 AGNs (representing a vastly greater actual unweighted number in the catalogue) and no cosmic
 342 rays, where one might expect about 2.6 (0.10×26). There may be a deficit here, although there
 343 is a 7% probability of recording no counts when 2.6 are expected. If the approximate distance-
 344 weighting factor (version b) is included, the overall features are not much changed. There are
 345 now 193 (weighted) AGNs, and 44 segments (those with AGN counts < 8) contain 102 of the 193
 346 AGNs, with $CR/AGN = 0.12$ in these, and 0.11 overall. But here, the proximity of the Virgo
 347 cluster increases its weighting and one expects 3.8 cosmic rays from that segment, where none
 348 is observed, which does look anomalous. In each segment of the plot in figure 3, the weighted
 349 number of VCV AGNs is given, and also (smaller figures) their weighted average distance in
 350 Mpc. The important segments with more than 6 weighted AGNs and at least one cosmic ray,
 351 in case (a) indicate 45 Mpc as the average distance — considerably further away than the Virgo

352 cluster (at 16 Mpc) — whilst the smaller $1/z$ -weighted averages in case (b) indicate a wide spread
 353 in the distance of AGNs in these segments, though not necessarily in the distance of the dense
 354 active regions. Some cosmic rays may originate beyond the 75 Mpc limit of the sub-catalogue
 355 used here. Two of the 21 cosmic rays have no AGN within the standard Auger window of 3.2° .
 356 Is their source further than 75 Mpc, or is the displacement more than 3.2° ? A technique for
 357 extending the correlation radius will be proposed in section 4. A more sophisticated treatment
 358 of sensitivity of the catalogue at different distances would be appropriate when more data are
 359 available.

360 The most striking implication of these correlations is that cosmic rays must come from very
 361 many sources (many 4° -spread circles being needed to cover the observations) within ~ 75 Mpc,
 362 and the most spectacular strong double-lobe radio galaxies do not supply a large part of them.
 363 Cen A supplies about 1/4 of the total extragalactic radio-source flux at 1.4 GHz, with M87 (Virgo
 364 A) about 1/5 of that, and Fornax A about 1/8 of Cen A's radio intensity. Biermann et al. [5] ex-
 365 pected these radio galaxies to dominate the cosmic ray flux if their jets are powered by the black
 366 hole spin, and suggested that intergalactic magnetic fields have displaced the cosmic rays from
 367 M87 very considerably, to give very many of the observed arrival directions along with the Cen
 368 A contribution (little displaced because of its proximity). A displacement of the Fornax A contri-
 369 bution was also proposed. However, if cosmic rays from M87 (Virgo A) were to be redistributed
 370 over the region containing the observed cosmic rays in the lower left hand quadrant of figure 1,
 371 scattering points randomly over a quadrilateral shape containing these observed directions shown
 372 in outline in figure 3b, only 27% of the points outside the galactic exclusion zone would have
 373 a VCV AGN within 3.2° . The observed correlation with AGN positions is too close: such a
 374 large-scale deflection is not supported, within the present statistics. Gorbunov et al [6] similarly
 375 propose a large extension of Cen A cosmic rays, but evidence is given in the following sections
 376 that magnetic deflections are small. Moreover, Gorbunov et al. drew attention to the importance
 377 of the huge $1/z^2$ geometrical factor favouring Cen A because its distance is only 3.4 Mpc. This
 378 gives it an advantage of a factor ~ 200 compared with the typical VCV AGNs at 40-50 Mpc
 379 that appear to be correlated with cosmic rays, so Cen A should at least match all the others as a
 380 source of local cosmic rays. If it does not, we have to suppose that particle acceleration to the
 381 highest energies is discontinuous, and Cen A is in its off state so far as 10^{20} eV is concerned,
 382 and the same may be true of Fornax A. It has been noted that there are two cosmic ray directions
 383 within 3.2° of Cen A, but these might well come from another double-lobed FRI radio galaxy,
 384 NGC 5090 (at 48 Mpc) in the list of Nagar and Matulich [3], and not in the VCV catalogue. This
 385 is within 1° of Cen A (see figure 1). The correlation of cosmic rays with these radio galaxies will
 386 be examined more quantitatively in section 5, but while figure 3 is before us, it can be seen that
 387 there is a close pair of cosmic rays near $\alpha = 331^\circ, \delta = 0^\circ$, in a very unremarkable segment of the
 388 diagram (1 or 0 weighted AGNs). The survey by Ghisellini et al. [12] also showed few normal
 389 galaxies here. There are not many AGNs in a further 50% of redshift either: is there a special
 390 object there? There is a BL Lac object with extended radio structure, PKS 2201+04, that Nagar
 391 and Matulich consider to be effectively an extended radio galaxy (see also [8]), though further
 392 away than the others, at 112 Mpc.

393 But why are no cosmic rays seen from the Virgo cluster region? Apart from any contribution
 394 from M87, the numerous other AGNs have as yet yielded no visible result, as remarked above.
 395 (a) Is it a technical problem of energy assignment or collection efficiency near the maximum
 396 zenith angle of 60° ? (b) Is the number of AGNs in the Virgo cluster exaggerated by the falling
 397 luminosity threshold for nearby AGNs in the catalogue, as referred to above? (c) Are the cosmic-
 398 ray sources not AGNs, but some other objects normally found near AGN but absent in the Virgo

399 cluster ? (d) Is cosmic-ray acceleration in Seyfert galaxies suppressed in a closely-packed envi-
 400 ronment? (e) Has the high density of gas generated a larger magnetic field in the supergalactic
 401 plane just here that deflects particles out of the plane (and out of our line of sight) and hides this
 402 source from us? Provisionally, it will be noted that option (b) is a distinct possibility, because, as
 403 noted above, the catalogue appears to have a bias crudely like a $1/distance$ to $1/distance^2$ effect.
 404 Such a progressive lowering of the power threshold at which AGNs are listed, as one moves to
 405 closer distances, may eventually move below the effective power threshold needed for cosmic
 406 ray generation, so that within some distance of Earth, many too-feeble AGNs are included in the
 407 catalogue. Zaw, Farrar and Greene [11] have favoured this explanation, noting that most Virgo
 408 cluster galaxies have bolometric luminosities below the values typical of other AGNs that corre-
 409 late with Auger cosmic rays. A better view would be obtained from more northerly observatories,
 410 which provides an incentive to devise more sensitive tests for AGN association.

411 In an earlier report [14] the Auger authors did make use of a uniform-exposure plot, but
 412 formed by distorting the declination scale of an Aitoff plot rather than a polar plot. This did
 413 display the anisotropy of the cosmic rays, though it conveyed the full information less clearly as
 414 it still suffers from the Aitoff distortions and discontinuities.

415 **4. A right ascension resonance: tracing the decoherence between the patterns of cosmic** 416 **rays and of their sources**

417 Is a 3.2° window the most suitable for seeking correlation between cosmic ray arrival di-
 418 rections and AGNs at different distances, in different parts of the sky, or at somewhat different
 419 energies? This is unlikely, whether this dimension arises from magnetic deflections or the size of
 420 galaxy or magnetar distributions, for example. Only the size and particular quality of the Auger
 421 data sample permitted a search for the optimal choice in their preliminary data set, and the best
 422 window size probably arose from its effect in reducing the confusion with background objects
 423 on the sky. For this reason, a correlation test that does not require a particular window size to be
 424 selected will be proposed, as an alternative technique for exploring the domain where this close
 425 association exists.

426 The notable feature of the cosmic ray directions in the original Auger report [1] was their an-
 427 gular closeness to AGNs. Hence a useful measure of association should be the angular distance,
 428 d_1 , between a cosmic-ray direction and the AGN nearest to that line of sight in a particular sub-
 429 set of the catalogue (such as a particular range of redshift). Here, d refers to the angular distance
 430 in degrees measured on the sky, and not to a distance on the uniform-exposure plot. Where $\langle d_1 \rangle$
 431 is the average value of d_1 for a set of observed cosmic rays, let this be used as a measure of their
 432 association with AGNs. This should be significantly less than $\langle d_1 \rangle_{rand}$ evaluated for a set of the
 433 same number of pseudo-random directions. (Here, “pseudo”-random means that random direc-
 434 tions are selected subject to weighting by the detector’s exposure to each part of the sky. They
 435 could be chosen using random points on the uniform-exposure plot, for example.) But what is
 436 “significant”? One would formally derive a probability, $P(\langle d_1 \rangle)$, that a random, or unrelated, set
 437 of directions would give such a low value of $\langle d_1 \rangle$, by simulating a very large number of “pseudo-
 438 random” sets, but it is hard to be sure that one has not inadvertently constrained the data in such
 439 a way as to produce a large error in $P(\langle d_1 \rangle)$, so such evaluations are always regarded with some
 440 degree of reservation. However, if the observed directions were put in the wrong position on the
 441 sky by a displacement $\Delta\alpha$ in every right-ascension angle, α , one would have a set of cosmic ray
 442 directions with the same detection efficiency, as this is independent of α . Figure 4 shows the
 443 average distance $\langle d_1 \rangle$ to the nearest AGN when the relative right ascensions of the cosmic rays

444 and the AGNs are shifted by $\Delta\alpha$ ranging from -180° to 180° . As just mentioned, for any value
 445 of the closeness measure $\langle d_1 \rangle$ the probability that a set of 21 pseudo-random directions will have
 446 a value at least as small as this can be calculated by Monte-Carlo simulation, and the values of
 447 $\langle d_1 \rangle$ at which this probability has the magnitudes 10^{-1} , 10^{-2} , .. 10^{-7} , are marked on the diagram,
 448 by dotted lines. The cosmic rays which are (before shifting α) within 12° of the galactic plane
 449 have not been used, as for the vital small shifts $\Delta\alpha$ they cannot be usefully compared with the
 450 AGN map.

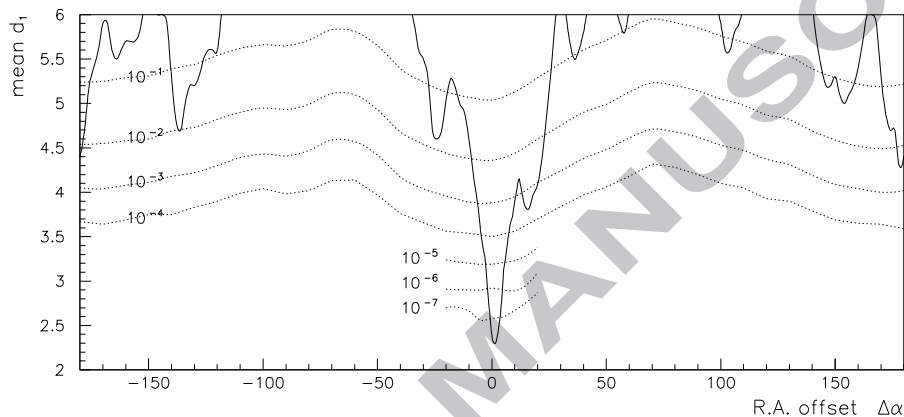


Figure 4: Right ascension resonance plot. Angular distance d_1 of cosmic ray direction from the nearest AGN ($z < 0.018$), averaged over the Auger set of 21 cosmic ray directions ($|b_{gal}| < 12^\circ$), plotted when the right ascension, α , of each AGN is shifted by $\Delta\alpha$. All angles in degrees. The near-horizontal dotted lines indicate the probability $P(\langle d_1 \rangle)$ of finding so small a value of $\langle d_1 \rangle$ in a set of 21 “pseudo-random” cosmic-ray directions at a specific offset position. (It varies with $\Delta\alpha$ because a 24° band almost devoid of AGNs is being shifted across the cosmic-ray pattern: only in the unshifted position does it coincide with the belt of omitted cosmic rays.) The preponderance of small distances d_1 soon disappears when the cosmic ray map and the AGN map are displaced slightly.

451 Only when $\Delta\alpha$ is close to zero is a clear association seen, with a chance probability $< 10^{-7}$
 452 — a sharp “resonance” in right ascension. Not only is a low P seen, but one knows where it
 453 should appear. There is much noise, far from the resonance, as a few cosmic rays happen to
 454 pass accidentally close to AGNs, but the clumpy nature of the AGN pattern results in occasional
 455 surprising false correlations, such as is seen in the Auger pattern with a displacement near 180° .
 456 These off-centre troughs are not really significant, as the marked probability P refers to the
 457 chance of observing such a low value of $\langle d_1 \rangle$ at one particular $\Delta\alpha$, so if a randomly-positioned
 458 trough is typically about 6° wide near its tip, there are about 60 positions available for accidental
 459 troughs, and multiplying the marked probabilities by ~ 60 gives an indication of the chance of
 460 seeing so deep a trough by accident somewhere: one is very likely to see a purely accidental
 461 trough reaching a level of $P = 10^{-1.8}$. A trough within a very few degrees of the centre is
 462 expected, however, so the marked probabilities apply directly there.

463 There is a complication, because this rotation in α moves the galactic exclusion belt which
 464 contains very few AGNs across the pattern of observed cosmic rays. It is undesirable to reclass-
 465 ify the cosmic rays as in or out of the galactic exclusion zone, as this changes the number of
 466 directions in the comparison, leading to several problems. For this reason, it has seemed prefer-

467 able to move the AGNs, leaving the cosmic rays fixed, but this still leaves the empty belt moving
 468 with the shifted AGN distribution (so long as we use the optically-detected VCV AGNs), so, as
 469 the same set of 21 cosmic ray directions is used at all times, some of the “nearest distances”, d_1 ,
 470 become appreciably larger for cosmic rays now falling in this belt. After testing several alterna-
 471 tive remedies, the disturbance that this causes seems to be best treated by limiting all individual
 472 cosmic-ray d_1 values to a maximum or “capped” value of 10° . Not only does this suppress the
 473 main effect of having a nearly-empty belt, but it also prevents the existence of one or two cosmic
 474 rays 25° from any AGNs (their source perhaps being at higher redshift) from raising the over-
 475 all $\langle d_1 \rangle$ by nearly a degree near the trough of the resonance. The movement of the empty belt
 476 of AGNs across the sky during this rotation causes changes in the probability of observing low
 477 values of $\langle d_1 \rangle$ by accident, as shown in the ups and downs of the dotted lines. Without the 10°
 478 cap, this variation is greater. In figure 4, $\langle d_1 \rangle$ at resonance is about 2.3° for the 21 cosmic rays
 479 in unobscured directions, whereas the average $\langle d_1 \rangle$ for pseudo-random sets of 21 is 6.8° , making
 480 the associated and unassociated populations well distinguished.

481 To estimate P at a particular shifted position, $\Delta\alpha$, of the AGN pattern, 100,000 “cosmic
 482 ray” points were selected randomly on a uniform-exposure plot, avoiding the 24° galactic exclu-
 483 sion zone, and the angular distance d_1 to the nearest (shifted) AGN was recorded for each. Then,
 484 a set of 21 samples was drawn from these 100,000, and $\langle d_1 \rangle$ calculated, up to 30 million such
 485 sets of 21 being produced, to find the frequency with which particular low values of $\langle d_1 \rangle$ were
 486 reached.

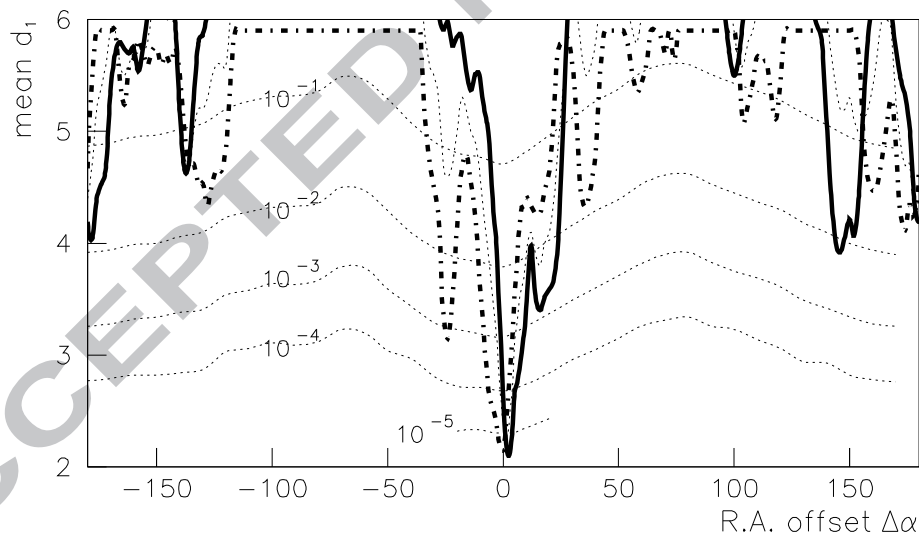


Figure 5: Right ascension resonance plot for subsets of the Auger data: (a) the first 10 cosmic rays $> 12^\circ$ from the galactic plane, used in choosing the selection cuts (thick dot-dash line), (b) the last 11 such cosmic rays, recorded after the cuts had been decided (thick solid line), and (c) all 21 such cosmic rays, repeated from figure 4 (thin dotted line). The dotted lines running across the diagram, showing the probability of reaching so low a value of $\langle d_1 \rangle$ at a specified $\Delta\alpha$, apply to the set of 11. See figure 4 for the probabilities applicable to a set of 21. The minima reached in subsets (a) and (b) have similar significance levels, in contrast to the probabilities of the numbers of 3.2° windows containing AGNs which was distorted in set (a) by the optimization process.

487 In the case of figure 4, the marked “probabilities” must be regarded with reserve, because the
 488 selection criteria for the data were not decided in advance. This $\langle d_1 \rangle$ resonance approach removes
 489 the relevance of window size, and this should remove the main source of bias, but the choice of
 490 maximum redshift for the test, and of energy threshold, might still influence the distribution in
 491 an accidental way in addition to the essential selection of the domain in which a real physical
 492 association exists. But to check that there is no essential difference between the first and second
 493 halves of the run (separated by the time at which the original cuts were determined), figure 5
 494 shows resonance plots for these smaller data sets. The thick dot-dash curve refers to the 10
 495 Auger showers from [1] outside the obscured zone of low galactic latitude that were observed
 496 before the selection cuts were chosen and which were used in making this choice; the thick full
 497 line applies to the 11 showers detected after this. The marked probability levels are for sets of
 498 11 pseudo-random directions, and would be slightly different for the smaller first set. Even with
 499 only 11 observed directions, a 10^{-5} probability level is reached (and the same is true for 10). In
 500 the first data set all 10 of the standard 3.2° windows around the cosmic ray directions contained
 501 VCV AGNs (within 75 Mpc); in the second data set the hit rate was 9/11. The thinner dotted line
 502 shows the curve for all 21 events, transferred from figure 4. For the nominal probability values
 503 P that apply in this case, see figure 4: they are roughly the square of the probabilities shown
 504 for a set of 10 or 11 directions. At $\Delta\alpha$ near 145° one can see an accidental dip at around the
 505 depth in “ P ” ($10^{-1.8}$) that was suggested above as likely to occur, but there are some other dips,
 506 usually also not significant, that are related to the effect of clumps of cosmic rays being moved
 507 across a clumpy AGN field, as they recur in both sub-sets, and at $\Delta\alpha$ near -25° there is one
 508 that is probably partly random. The resonance technique could thus detect strong associations
 509 with AGN patterns in fairly small data sets, even when the best window size is not known. The
 510 main conclusion from figure 5 is that the association between the cosmic rays reported in the
 511 Auger paper and the VCV AGNs on a scale of a few degrees are very highly significant, and not
 512 generated accidentally by the optimization process.

513 Four other applications of this right-ascension resonance will be considered. First: as the
 514 technique can reveal such associations in data sets smaller than that of the Auger Observatory,
 515 do associations with AGN directions appear in data of other experiments, viewing the northern
 516 hemisphere? This raises difficulties which are mentioned below, and the real lessons to be learned
 517 are still being explored. Second: how significant are the associations with a different list of target
 518 objects — the extended radio galaxies put forward by Nagar and Matulich? Third: can one detect
 519 systematic displacements in the directions that could be caused by magnetic fields? Fourth: can
 520 one explore how far in redshift the Auger association persists, to check the significance of the
 521 apparent 75 Mpc limit, and use the position of the GZK horizon to check the energy of the
 522 particles?

523 As already remarked, the proportion of Auger cosmic rays to VCV AGNs appears to be
 524 lower than usual in the region of the Virgo cluster, long assumed to be an important local source.
 525 The HiRes observatory was well placed to observe this region, but reported seeing no cosmic
 526 ray excess in that direction, and indeed no association of cosmic rays above 56 EeV with VCV
 527 AGNs², using the Auger windows. Would some other window size have been more appropriate?
 528 Abassi et al. [10] estimated that the energies attributed by Auger to cosmic ray particles were
 529 too low by 10% (which is quite possibly an underestimate of the difference, as it depends on the
 530 energy at which a comparison is made), compared with the HiRes scale, from a comparison of

²56 EeV being the earlier estimate of the Auger threshold

531 energy spectra, and so they picked out a sample of cosmic rays for comparison having energies
 532 above (1.1×56) EeV on the HiRes scale. There were 13 HiRes events supposedly above 56
 533 EeV on the Auger scale [10, 15], and a resonance plot for the 10 outside the galactic obscuration
 534 zone is shown in the upper panel of figure 6. The probability estimate is somewhat approximate,
 535 being based on the declination distribution of stereo events above 10 EeV [16]. There is no signal
 536 at $\Delta\alpha = 0$, in conformity with their paper [10] finding no correlations with AGNs. The single
 537 trough near -155° is a little unusual, though its probability level is near that of the peculiar dip
 538 seen on the full-sample Auger plots near 180° , but with a different sample size. (The events were
 539 displayed on a sky map in [10], but the positions used here were those tabulated on their web-site
 540 [15], which seem to be consistent with the map.) If a uniform-exposure polar plot is made (as
 541 appropriate to the HiRes observing conditions) there is no tendency for the cosmic rays to be less
 542 numerous in the segments which have few (weighted) AGNs ($z < .018$), unlike what was seen
 543 in figure 3: the cosmic rays here do not follow the AGN pattern even on a large scale. Is this
 544 astonishing disappearance of any AGN connection a feature of the northern celestial hemisphere
 545 — or a surprisingly sharp change with energy that is not fully taken out by the 10% difference
 546 assumed in the energy scales used in the two experiments? This has to be considered as there
 547 must be a rapid change in Auger's sky distribution just below 57 EeV because the optimization
 548 process found that the significance decreased if the energy threshold was decreased despite a
 549 very rapid increase ($E^{-3.5}$ integral spectrum) in the number of events available, but a list of
 550 Auger events below 57 EeV has not been published.

551 The much earlier experiment at Haverah Park pioneered the particle detector technique used
 552 at the Auger Observatory, and viewed the northern sky. Using the energy estimation methods then
 553 current, this experiment had 13 showers above 70 EeV – but revised to ≈ 50 EeV [17] with more
 554 modern shower models – 11 of them outside the galactic exclusion zone ([18] with $\theta_{max} = 45^\circ$),
 555 and a resonance plot for these cosmic rays, again matched against the VCV AGNs within 75
 556 Mpc, is shown in the lower panel of figure 6. There is an apparent resonance with AGNs, with
 557 a 2% chance of being an accident. But the true energy threshold of these Haverah Park cosmic
 558 rays cannot be 50-70 EeV, judging by the flux, because the exposure was only several percent
 559 of Auger's: the energy must be well below the 57 EeV at which the AGN correlation appears
 560 in the Auger observations, and thus very many of these cosmic rays will originate beyond 75
 561 Mpc, so the dip at 0° is less deep. An interesting feature is that if 3.2° windows are drawn
 562 around the 11 shower directions, one of them contains 12 VCV AGNs (rather than the typical
 563 1.1), being aligned within 1° of M87 at the centre of the Virgo cluster, and if the AGN count is
 564 extended to 130 Mpc, another window contains 14 AGNs, being aligned within 3° of a cluster
 565 ($\alpha = 262^\circ, \delta = 58^\circ$) at 117 Mpc. This suggests that the Virgo cluster is not completely inactive
 566 as a source, and disfavors the possibility that its output is disguised by a large local magnetic
 567 deflection.

568 Investigation of the most reliable way to detect associations and estimate energy in such
 569 datasets is at an early stage, and the result will be reported separately, but a comparison of
 570 these three experimental results suggests that the 57 EeV threshold for association with nearby
 571 AGNs, found by Auger, may not be a simple marker of the point at which interactions with the
 572 microwave background radiation limits proton survival to about 100 Mpc. The depth of shower
 573 maximum measured by Auger [19] indicated that, unexpectedly, the particles become heavy, and
 574 hence highly charged and strongly deflected, as 50 EeV is approached, though it is not clear that
 575 this was the case below 30 EeV. This may be the only way to understand a wide spread of arrival
 576 directions in the HiRes data, if the fluorescence technique favours heavy nuclei rather more than
 577 does the array of water tanks (i.e. assigns them a slightly higher energy). The Haverah Park

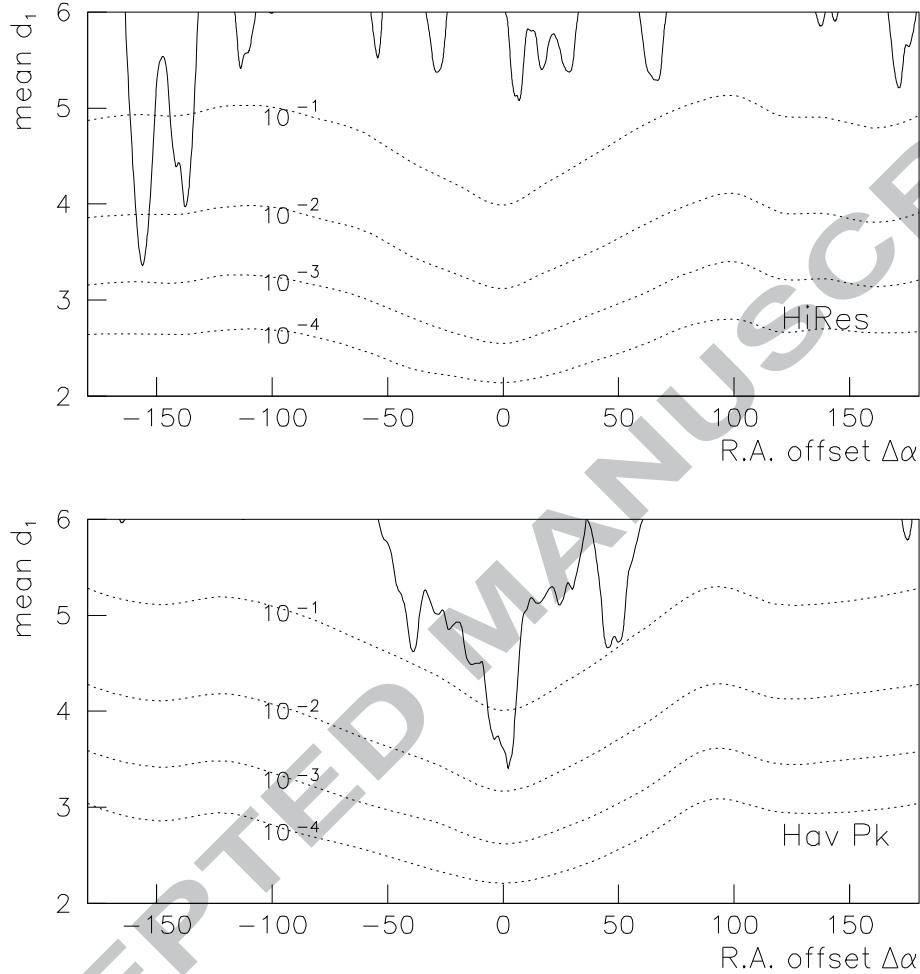


Figure 6: R.A. resonance plots for northern hemisphere observations: cosmic rays $> 12^\circ$ from galactic plane. Upper: HiRes: 11 cosmic rays estimated to have energies above 56 EeV on the Auger energy scale [10, 15]. Lower: Haverah Park: 11 cosmic rays [18] originally estimated to have energies above 70 EeV, but possibly about half that.

578 array did not find an expected GZK turn-down in the primary spectrum (as also AGASA, even
 579 more strikingly): the apparently most energetic particles were presumably the badly-measured
 580 ones that suffered large fluctuations in their energy assignment; and were probably thus protons.
 581 (The Haverah Park events also occurred in a somewhat lower energy domain, possibly before
 582 the highly-charged nuclei had become so important.) Why should these problems with energy
 583 assignment for individual proton showers not occur also in the Auger data? In that case, the
 584 domain above 57 EeV apparent energy may be where an accidental tail of proton showers, which
 585 retain good directional information, emerges above the highly deflected component of heavy
 586 nuclei. The 57 EeV threshold would then be to a large extent an accident of technique (and

587 an upper limit of the heavy nuclei), and the AGN signal might be highly dependent on shower
 588 selection. A method for rejecting heavy nuclei on the basis of the detector signals would be
 589 highly desirable.

590 **5. Correlations with extended radio galaxies**

591 There is a much smaller alternative catalogue, of large radio galaxies, against which the
 592 cosmic rays can be compared, which is equally significant, at the one-in-a-million level, may
 593 be virtually independent of selection-optimization bias, and is undoubtedly plausible, a priori.
 594 This is the set of 10 “extended radio galaxies” listed by Nagar and Matulich [3] as being within
 595 the declination range observable by Auger and the redshift range selected for the Auger analysis
 596 ($z < 0.018$). Nearly all are classified as probable FRI radio galaxies, except for Fornax A. These
 597 authors considered objects included in Liu and Wang’s [20] catalogue of galaxies with radio jets,
 598 and selected those for which the radio map showed emission whose total extension on the two
 599 sides added up to more than 180 kpc (scalar sum). Only three of these galaxies are on the VCV
 600 list of optically-detected AGNs — NGC 4261 (3C270), Cen A and Cen B, the latter being very
 601 near the galactic plane, although there is now no need to exclude the zone of low galactic latitude
 602 when comparing cosmic rays with radio galaxies, which shine through the dust. M87 does not
 603 meet their selection test. Concentrating first on the statistical argument, of 27 cosmic rays, 4 have
 604 at least one of these 10 radio galaxies within a “standard” 3.2° window; yet the average particle
 605 from an isotropic flux would have 0.0015 such encounter by chance, and there is well below a
 606 10^{-6} probability of having 4 “hits” in a sample of 27 particles. As the selection conditions were
 607 not optimized for these targets, this appears to be an essentially independent demonstration that
 608 the cosmic rays are far from isotropic and truly associated with certain AGN-type objects (and
 609 the argument would be little affected if one removed the two galaxies that appeared in both lists
 610 and had nearby cosmic rays). The chance of having so many hits by accident is still under 1 in a
 611 million if directions are not chosen randomly but from a broad region of the sky corresponding
 612 to the cosmic-ray pattern in figure 1 but smeared out by 30° rms spreading (in all cases the
 613 acceptance efficiency of the detector is taken into account). So the radio galaxies themselves do
 614 offer a pattern significance test essentially independent of the VCV association test. But a 3.2°
 615 window for counting associations is really too small for this situation in which the targets are
 616 less crowded on the sky, as will shortly be seen, so a $\langle d_1 \rangle$ resonance plot is shown, to check this
 617 level of significance, before moving on.

618 Figure 7(a) shows the mean distance in degrees of the 27 cosmic ray directions to the nearest
 619 of these 10 “extended radio galaxies”, as the right ascension of the objects is shifted, and plot
 620 (b) shows the same but in the next 50% extension of the redshift range (0.018 to 0.027), using
 621 the two further radio galaxies that Nagar and Matulich note, at positions ($\alpha = 52.7^\circ, \delta = -3.1^\circ$
 622 on figure 1, 85 Mpc) and at 112 Mpc ($\alpha = 331.1^\circ, \delta = +4.7^\circ$). As these authors do not state
 623 whether there were any more similar galaxies in this range, there is some uncertainty about the
 624 full interpretation of this second plot, a subject that will be raised again when considering source
 625 distances in section 7. (Because the density of target galaxies is so low in this catalogue, the
 626 random separations are larger, and the angular distances d are capped at a value of 13° rather
 627 than 10° in forming the averages for these plots, though present results are insensitive to the
 628 precise value chosen.)

629 Without making a choice of window size, the significance of the association (case a) is not
 630 quite the same as quoted above using a “standard” size of window, but this is of no practical
 631 consequence.

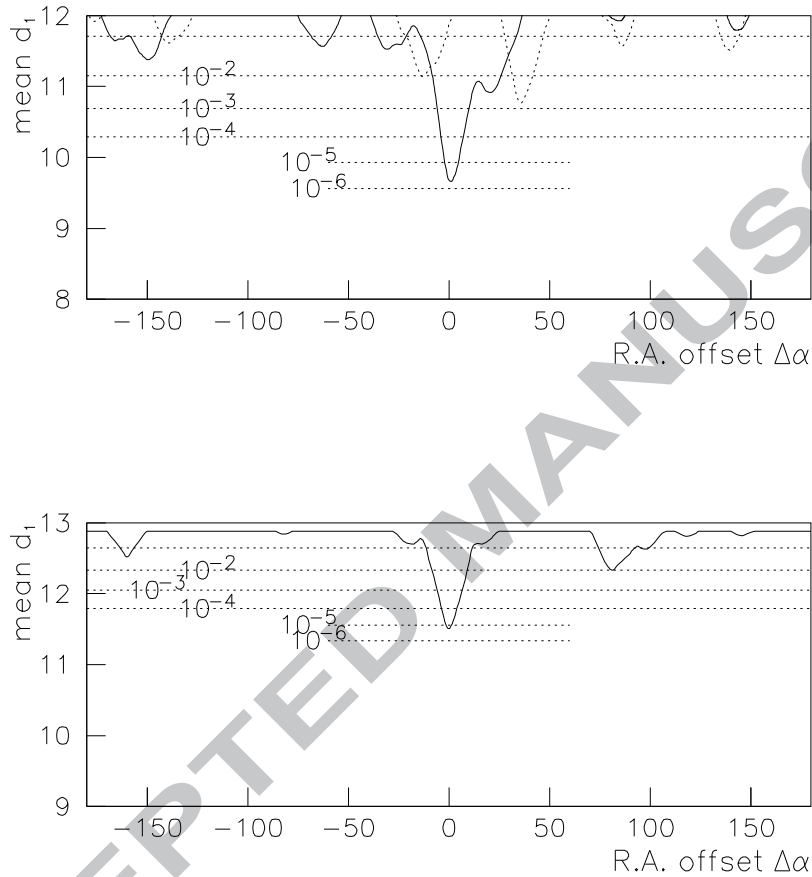


Figure 7: Association between the 27 Auger cosmic ray directions and the directions of extended radio galaxies listed by Nagar and Matulich. The mean distance between the cosmic ray and the the galaxy nearest on the sky is again measured in degrees. (a, upper panel) The 10 “extended” radio galaxies within 75 Mpc are considered; (b, lower panel) the listed radio galaxies (only 2) in the next 50% range of distance are used. The probability lines do not waver in level because there is no special galaxy avoidance zone moving across the sky now, for radio galaxies; but in case (b) the probabilities should not be relied upon, as the unbiased selection of the galaxies in this case is uncertain. (a) also shows, dotted, the resonance curve (but not the probabilities) for the radio-jet galaxies listed by Liu and Zhang that do not have extension greater than 180 kpc: they do not show a strong signal near 0° .

632 These extended radio galaxies were selected from a list of galaxies with radio jets [20]. Are
 633 the other jets also effective sources? Omitting the (few) cases with short jets, with total length
 634 less than 1 kpc, the galaxies selected as having extended lobes comprise about 40% of the total in
 635 the localities considered here. A $\langle d_1 \rangle$ resonance curve for those that were not selected by Nagar
 636 and Matulich, shown dotted in figure 7a, shows no dip at $\Delta\alpha = 0^\circ$, indicating that they are not

637 more strongly associated with cosmic rays than are the typical VCV AGNs.

638 It may be wondered how one finds room for more sources of these cosmic rays when almost
639 all of them have been associated with optical AGNs, above. The explanation is, as remarked in
640 section 2, that the close grouping of AGNs in clusters normally prevents identification of what
641 object within a few degrees is the true source, which could be an object belonging to the cluster
642 but not in the VCV catalogue. Most radio galaxies are such objects, and if they are indeed
643 particularly efficient sources, we may in this case be able to identify the actual galaxy that is the
644 source.

645 The usual 3.2° window size must be expected to exclude many cosmic rays if they do typ-
646 ically have rms spreads of $\sim 4^\circ$ around the VCV AGNs, and the counting window can safely
647 be extended to 6° for greater counting efficiency when there is such a small density of targets
648 on the sky: 4 more hits then appear, and there is no indication that one is picking up accidental
649 pairings, although there may be a contamination from cosmic rays generated by other weaker
650 sources in the surrounding cluster. In contrast with the VCV optically detected AGNs, which
651 typically had ~ 0.1 cosmic ray associated (see the discussion of figure 3), the ratio is close to 1.0
652 now: there are 12 cosmic rays that have at least one of these 12 extended radio galaxies within
653 6° (counting out somewhat beyond $z=0.018$ now), even though about 2 of these 12 cosmic rays
654 could be attributed to surrounding VCV AGNs if they are contributing 0.1 each. Four of these
655 radio galaxies have no associated cosmic ray (Fornax A, 25 Mpc, NGC 3557, 43 Mpc, NGC
656 4261/3C270, 31 Mpc and NGC 4760, 66 Mpc), and it now seems likely that there is a fifth —
657 Cen A. NGC 5090 (at 48 Mpc) has three cosmic rays within 6° , and so has Cen A (3.4 Mpc)
658 which is so nearly aligned that both these galaxies appear in the same events. As Cen A has an
659 advantage of ~ 200 in its $1/distance^2$ factor relative to most of the other typical emitters con-
660 sidered here, but does not overwhelm them, it is probably in an “off” state, and the three cosmic
661 rays seemingly associated with it are then more logically attributed to NGC 5090. Other radio
662 galaxies seem to have two cosmic rays within 6° — Cen B (at 54 Mpc), Markarian 612 (83 Mpc)
663 and CGCG 403-019/PKS 2201+04 (112 Mpc) — though in some cases weaker sources in the
664 cluster may perhaps contribute one. I am quoting the distances given by Nagar and Matulich.
665 As so many contribute more than one, the 5 undetected suggest that either the emission is not
666 continuous, or that the maximum energy is lower for some of them. The Nagar and Matulich
667 galaxies should be seen to associate with cosmic rays again in future Auger exposures.

668 In [3] it was proposed that these FRI galaxies were the essential sources, and that the re-
669 maining cosmic rays (perhaps 17 out of 27 from the figures above) were probably not really
670 associated with VCV AGNs, and were approximately isotropic. The authors also remarked that
671 the correlation with VCV AGNs must be distorted by the inclusion in the catalogue of bright H2
672 galaxies that were originally mistaken for AGNs. Their suggestion has been tested by plotting a
673 resonance curve for a reduced cosmic ray sample (having removed those which pass within 6°
674 of Nagar-Matulich galaxies), and measuring their angular distances from the objects remaining
675 in a reduced VCV AGN catalogue for $z < 0.018$ (having removed the 3 specified radio galaxies,
676 and also the H2 galaxies as suggested). The result, plotted in Figure 8, shows that these cosmic
677 rays that are not seen to be associated with the radio galaxies are not isotropic: there is still a
678 pronounced trough close to 0° , with the chance that it arises by accident below 10^{-4} , still a very
679 significant association.

680 One merit of the VCV AGN catalogue is that it contains the right density of objects to provide
681 correlations with a large proportion of individual cosmic ray directions, but not so many as
682 to make this correspondence unavoidable even with random directions, so it makes a striking
683 demonstration of a close association with cosmic rays numerically possible if it exists. It has been

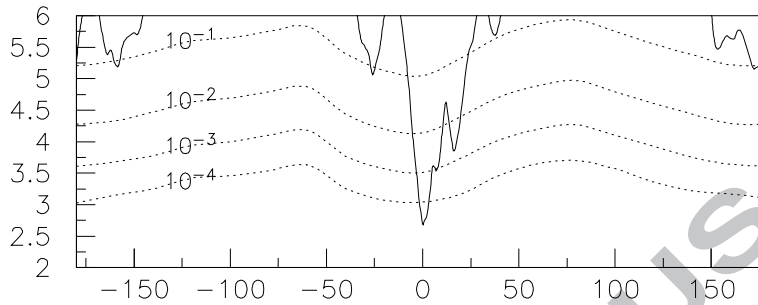


Figure 8: Figure 8. Plot of $\langle d_1 \rangle$ against R.A. shift $\Delta\alpha$ for cosmic rays which do not correlate within 6° with extended FRI radio galaxies (16 of the original 21 cosmic rays), compared with the positions of VCV AGNs after removing H2 galaxies (not true AGNs) and the extended radio galaxies from the list, to test a suggestion of residual isotropy by Nagar and Matulich [3]. The reduced set of cosmic rays still shows a strong association with the directions of optically detected AGNs.

684 argued above that this close association, very surprisingly, does exist, and is very significant even
 685 when allowance is made for the selection data cuts which optimized this correlation in the first
 686 half of the data-taking period. If one were to look to greater distances, however, source confusion
 687 would mount: there would be multiple close AGNs for many cosmic rays, confusing the picture
 688 quite apart from the need to allow for the opposite problem of serious catalogue incompleteness.
 689 The class of radio galaxy discussed above would be much more suitable than VCV AGNs to
 690 trace the extension of cosmic ray sources beyond 75 Mpc, because their number density is low
 691 enough to avoid source confusion, and the catalogue will not suffer from incompleteness until
 692 greater distances are reached. The X-ray selected AGNs in the Swift BAT catalogue might also
 693 be useful in this way, and George et al. [7] have already suggested that a correlation appears to
 694 extend to about 100 Mpc.

695 Thus it appears that both FRI radio galaxies and Seyfert galaxies can accelerate protons to
 696 10^{20} eV, though the latter have a lower output. It seems that an intense hot-spot, as seen at the
 697 termination of FR II jets, and anticipated as a promising acceleration site [21, 5], is not implicated.
 698 If these two classes of active galaxy make up the relevant accelerators, the acceleration site may
 699 possibly be nearer to the base of the jet.

700 6. Magnetic deflections

701 If 3° of the spread of proton arrival directions around their sources represents a deflection in
 702 varying magnetic fields in travelling ~ 45 Mpc, an effective transverse magnetic field $\approx 0.1nG$
 703 would produce this. If the field changed randomly on a scale of L Mpc, a typical total field
 704 strength in each domain of $\approx 1.6nG/\sqrt{L}$ would be required. This must be an upper limit, as there

705 will be other factors contributing to the scatter. A systematic deflection caused by a net average
 706 field normal to the line of sight might be detected by a shift in the position of the “right ascension
 707 resonance” from its expected position at $\Delta\alpha = 0$ — if the field had a component parallel to
 708 the earth’s rotation axis. But other field directions can be investigated by shifting the AGN
 709 pattern in some other direction on the sky by choosing a different axis for the pattern rotation.
 710 The resonance effect has been examined when the “AGN sky” is rotated through small angles
 711 about the galactic pole or about an axis perpendicular to this (i.e. in the galactic plane, chosen
 712 to be at a galactic longitude of 45° so as to be nearly perpendicular to the main concentration
 713 of cosmic-ray directions). Of special interest is the set of AGNs at positive galactic latitude,
 714 seen on the left hand side of figure 1, for these 9 at galactic latitude $> 12^\circ$ are mostly grouped
 715 in a small part of the sky and so may travel through a similar magnetic field. On rotating the
 716 AGN sky about the special axis normal to the galactic pole, which is also about 90° from the
 717 majority of these 9 directions, no perceptible shift from zero in the position of the resonance was
 718 seen (Figure 9c), although this plot is very noisy, and a much larger data set may be needed to
 719 make clear what is happening. But if a rotation about the galactic pole is made, thus shifting
 720 the AGNs parallel to the galactic plane, they are seen to need an offset in order to match the
 721 cosmic-ray directions. To make the sampled region of sky more well defined, two outlying
 722 cosmic rays may be omitted (one at much smaller galactic longitude than the others, and one at
 723 the high latitude of 54°), leaving a more compact group of 7 arrival directions whose centroid is
 724 at galactic longitude 308° and latitude 24° . The resonance curve (figure 9b) shows that the AGNs
 725 best match the cosmic ray directions when offset by about 4° parallel to the galactic plane. (A
 726 shear was applied in these rotations, as described in the next paragraph.) This sky rotation about
 727 the galactic pole tests any deflection of cosmic rays parallel to the galactic plane (due to a “ B_z ”
 728 field component, perpendicular to the galactic disc), whilst the previously mentioned rotation
 729 tests any displacement perpendicular to the galactic plane, due to a field component parallel to
 730 the plane (though cylindrical symmetry of the galaxy may tend to make the averaged field along
 731 the line of sight nearly cancel out in this case, where no displacement effect was found). No
 732 clear offset was seen if the other 12 (negative latitude) cosmic rays were used (figure 9a). These
 733 directions are more widely scattered, and typically further from the galactic plane, where the
 734 average galactic field strength might be considerably smaller.

735 A rotation of the AGN pattern about any axis, such as the galactic polar axis, produces a
 736 smaller actual displacement on the sky as the “pole” is approached. Since the actual displacement
 737 of cosmic rays was of prime interest in this part of the investigation, a “shear” was applied to the
 738 rotations described in this section: any AGN was displaced in longitude, λ , by $\Delta\lambda = \omega \cdot \sec\phi$,
 739 where ϕ is the latitude, rather than all by the same $\Delta\lambda = \omega$, thus having the same actual shift
 740 ω on the sky for each AGN, making it easy to read off the displacement of the particle. The
 741 terms “longitude” and “latitude” here relate to the particular axis of rotation that is being used.
 742 (A rather similar curve, but without such a large sideband noise is obtained in the case 9(b) by
 743 rotating in right ascension instead of in galactic longitude, as in this region of the sky the two
 744 directions are not very different.)

745 Such a deflection of 4° by the galactic magnetic field would be quite compatible with the
 746 range of expected values shown in figure 8b of Abraham et al.[1], and would correspond to a field
 747 directed “down” towards the galactic disc, with a strength integrated along the particle’s path of
 748 $6\mu\text{G} \times \text{kpc}$, if the particles are protons — say, $0.3\mu\text{G}$ on average over 20 kpc. The trajectory
 749 passes about 2 kpc above the galactic plane at about 7 kpc from the Galactic Centre. Since
 750 deflections, at a known energy, will be proportional to nuclear charge, the particles are surely
 751 not very much more highly charged than helium nuclei, and at this energy are very unlikely to

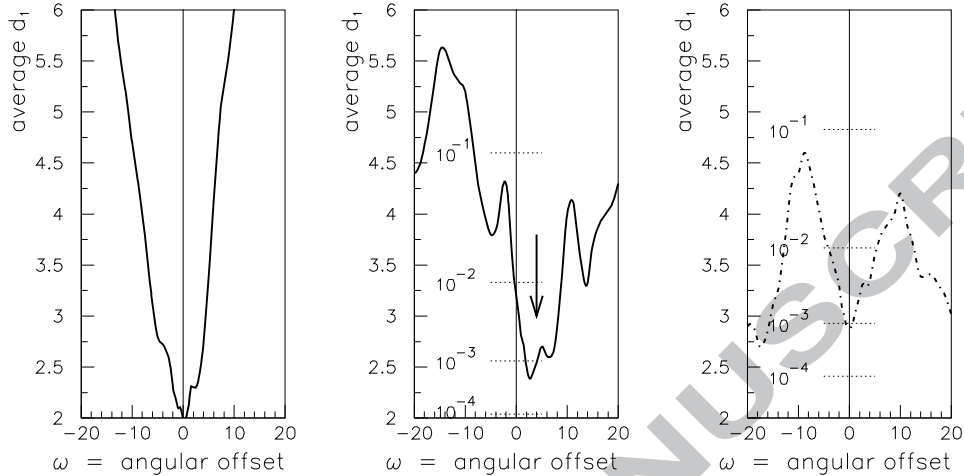


Figure 9: Position of the resonance between Auger cosmic-ray directions and the AGN positions ($z < 0.018$) when the AGN patterns are shifted in a direction related to galactic coordinates: in (a) and (b), the AGN positions are shifted by an angle ω parallel to the galactic plane, and in (c) by an angle ω perpendicular to the plane (see text). (a) uses the 12 cosmic-ray directions with galactic latitude, $b < -12^\circ$; (c) uses the 9 which have $b > 12^\circ$. (b) uses 7 of the latter 9, which arrive from a relatively limited part of the sky around the direction ($l = 308^\circ, b = 24^\circ$). In case (b), where the particles have passed just above the galaxy, they appear to have been deflected by about 4° , as though by a B_z component of the galactic magnetic field.

752 be helium nuclei, as these survive only about 1 Mpc in the microwave background. Of course,
 753 not having enough data to treat several different parts of the sky separately, the magnetic field
 754 cannot be separated from a metagalactic field of $6\text{nG} \times \text{Mpc}$. There may well be a significant
 755 metagalactic contribution seen in the widespread random $3 - 4^\circ$ scatter discussed previously, as
 756 the systematic shift was only seen for a particular set of directions, at the rather low galactic
 757 latitude of 24° . The value of extending these tests to a larger data set is clear.

758 A 4° displacement of the resonance of course implies some changes in the list of which AGNs
 759 appear in 3.2° windows around the cosmic ray directions. With this special group of 7 cosmic
 760 ray directions there are still 2 empty windows (to 75 Mpc), but the number of AGNs in the 5
 761 active windows is increased — so it may not yet be convincing that there must be a magnetic
 762 deflection. There now appear 9 AGNs in the standard windows around revised “undeflected”
 763 cosmic ray directions, instead of 5 in the original list. Cen A now appears in only one window
 764 rather than 2, but one of the new AGNs brought in is the FRI AGN IC 4296 on Nagar and
 765 Matulich’s list [3], which now has a distance d of 0.4° instead of 3.8° .

766 7. Correlations with AGNs in different distance ranges

767 The Auger AGN study [1] found that the correlation was most significant when only the
 768 AGNs having redshift $z_1 = 0.018$ (distance < 75 Mpc) were used. This would have important
 769 implications, discussed in the next section. However, a maximum significance with a redshift
 770 limit of z_1 does not mean that there are few cosmic rays from beyond this limit; so direct infor-

771 mation on the distances of travel of the detected cosmic rays should be sought. Three approaches
772 to this tricky problem will be sketched here.

773 (1) Looking for coincidences (within 3.2°) with VCV AGNs at different distances is not
774 helpful in a very straightforward way, as these objects are so numerous that a typical cosmic ray
775 direction eventually matches AGNs at different distances. This is shown in table 3, where, in the
776 line labelled $z \text{ “.000-.017”}$, the 21 cosmic rays outside the galactic obscuration zone are shown
777 in the sequence of their detection, with “x” showing that the particle matched an AGN in this
778 distance range (i.e. the cosmic rays discussed previously), and “.” signifying that there was no
779 match: there were 19 “hits”. The following two lines similarly record whether these same 21
780 cosmic rays matched AGNs in the next succeeding ranges of redshift, each 50% as large as the
781 first.
782

AGN redshift		
.000-.017:	x x x x x x x x x x x x x . x x x x x x .	19
.018-.027: x x . . x . x x .	5
.028-.035:	. . . x x . x . x . x x . . x . . x x . x	10

Table 3: Sequence of cosmic rays matching AGNs (see text).

783 The point of origin of the particle is obviously not determined unambiguously: a line of
784 sight can pass within 3.2° of more than one AGN. The dividing line in the sequences shown in
785 table 3 marks the end of the “first half” of the run, at which point the initial selection cuts were
786 optimized. Although the 3.2° window size used here results from a re-optimization at the end of
787 the run, so the first half should not necessarily look anomalous, this point of decision was made
788 when a pre-defined level of significance was reached, so an atypical sequence may have been
789 recorded at this point for this reason — and the 10/10 hit rate in the initial period may hence
790 be distorted. The 9/11 hit rate after this is close to what would be expected if cosmic rays do
791 arrive from directions having 3.5° rms scatter around VCV AGNs: it was found that 77% of
792 particles should then have an AGN within 3.2° along the line of sight. Such simulations also
793 show that 21 particles originating in the near zone, $z < 0.018$, would typically score 12 hits
794 in the second and third distance zones, not very different from the 15 recorded, so that there
795 are probably not very many particles originating in these more distant zones (though several
796 associations could be missed because the VCV catalogue will become significantly incomplete
797 there). A more elaborate study of this limited sample suggests that (because of the high hit-rate
798 in the first line) most particles originated within 75 Mpc, but very crudely 0-25% might come
799 from sources beyond 75 Mpc, though a more precise estimate cannot be made.

800 (2) Resonance plots can also be used to study the extent of the correlation with increasing
801 distance, as they are not dependent on window size, though the plots are disappointing. Right
802 ascension resonance curves for the 21 Auger cosmic rays are shown in figure 10 for $\langle d_1 \rangle$ using
803 angular distances to the nearest AGN listed in particular redshift ranges of the VCV catalogue:
804 (a) $z < 0.018$, (b) 0.018-0.027, (c) 0.028-0.036. It is at first disconcerting to see that although
805 most of the published cosmic ray directions (in unobscured regions) align closely with AGNs
806 within 75 Mpc, as discussed above, and as shown in figure 10a, they also have a (much less
807 significant) alignment with AGNs between 116 and 150 Mpc (figure 10c). Although this is
808 somewhat like the results for window hits listed above, it is surprising that the 116-150 Mpc

809 group shows a small apparent resonance near $\Delta\alpha = 0$ (that was not seen in the simulated curve,
 810 below). To extract the information on distance of origin, the best that can be done at present is
 811 to model the correlations one would get if the observed cosmic rays originate in a specific range
 812 of distance. So, for this purpose, I have assumed that cosmic rays originate as though from any
 813 VCV AGNs, are scattered with a characteristic spread, and that at greater distances a decreasing
 814 fraction of the AGN's output is seen, because GZK energy losses allow us to receive only those
 815 particles emitted above an energy threshold which is increasingly above 57 EeV for more distant
 816 sources. The Auger sample has an energy spectrum above 57 EeV which may be represented by
 817 $j = (E_{max} - E)/(E_{max} - E_o)$, where j is the fraction of particles above energy E , $E_o = 57$ EeV,
 818 and $E_{max} \approx 92$ EeV. This ignores a single particle of energy well above 92 EeV, which is of no
 819 consequence in this context.

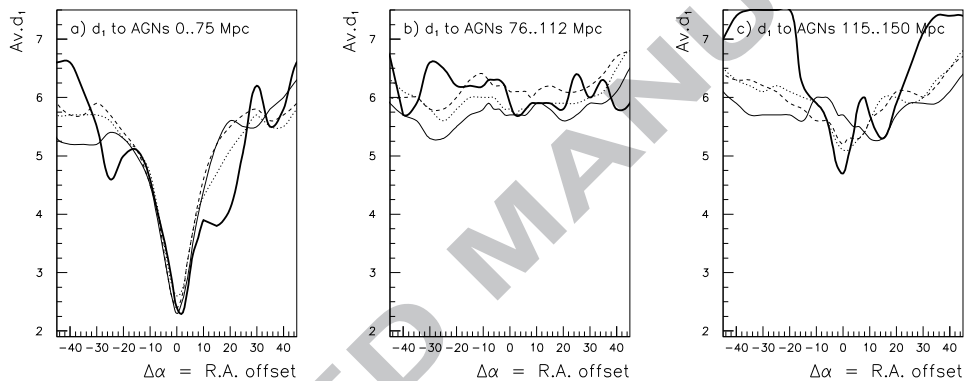


Figure 10: Right-ascension resonance plots for the 21 Auger cosmic ray directions not near the galactic plane. The mean distance to the closest VCV AGN (d_1) is plotted against shift $\Delta\alpha$ in right ascension of AGNs by the thick lines, (a) for AGNs in redshift range < 0.018 , (b) $0.018-0.027$, (c) $0.028-0.035$. The thinner full, dashed, dotted lines show the average curves found in models in which the cosmic rays are emitted from the vicinity of VCV AGNs, with detectable output reduced by a factor falling to zero at redshift z_{max} in the range 0.018 to 0.025 (see text). When z_{max} exceeds 0.024 , approximately, the correlation with the closer AGNs, noted by the Auger report, weakens. The seeming correlation with AGNs at $z > 0.027$ appears to stem in part from accidental alignment of AGN clusters.

820 Assuming the local spectrum does not vary much with position in space, it might be treated
 821 roughly as though E_{max} , above, is the maximum energy with which most particles are generated,
 822 and that particles cannot be received here from sources more distant than D_{max} (redshift z_{max}),
 823 corresponding to the distance over which protons lose an amount $\Delta\log_{10}E = 0.22$ (falling from
 824 92 to 57 EeV). This effect is modelled approximately by multiplying the output of any AGN at
 825 redshift z by a factor $(1 - (z/z_{max})^2)$ to represent the decreasing fraction of its particle output that
 826 remains above 57 EeV by the time it reaches us. (“92 EeV” was quoted merely in explanation:
 827 no energy value is used at this stage, but only a parameter z_{max} .)

828 Varying z_{max} (and the rms spread of cosmic rays around source AGNs) to get a crude fit to
 829 the resonance trough, $\langle d_1 \rangle$ near $\Delta\alpha = 0$ in the three redshift zones out to 0.036 , the best fit was
 830 with $z_{max} \approx 0.023$ and slightly favours a scatter varying with \sqrt{z} (rms being 3.5° at 45 Mpc)
 831 rather than being constant. Models with $z_{max} = 0.018, 0.0216$ and 0.0252 gave the resonance
 832 curves shown by various thin lines in figure 10. The present rough models and low statistics

cannot give accurate fits, but if z_{max} is increased further the trough becomes less deep in the comparison with AGNs in the nearest redshift zone, < 0.018 (figure 10(a)), that was picked out by the Auger authors. A range z_{max} of 0.023 corresponds to a maximum source distance of 96 Mpc if $H_o = 72$, a travel time of close to 300 Myr. When better statistics are available and refitting is attempted, the distance-dependence of the selection bias for VCV AGNs should be investigated, although it would be unlikely to have much effect on a “cut-off” point.

(3) The alignment of cosmic rays with extended radio galaxies offers a much better chance to investigate the source distances, as multiple alignments for a cosmic ray will rarely occur, apart from the special case of Cen A and NGC 5090. The shaded histogram in figure 11 shows the numbers of such galaxies (as listed by Nagar and Matulich) found in 20 Mpc intervals of distance, but the lightly shaded part reaching as far as 120 Mpc contains objects that seem to have been added because they were seen to align with cosmic rays, and may not be a complete sample in this region. To indicate how the radio-galaxy distribution may be expected to continue, the total number of galaxies with radio jets, listed by Liu and Zhang [20], excluding those with total jet length less than 1 kpc but without any selection based on extension of lobes seen in radio images, is shown by the line, the scale being shown on the right. Below 80 Mpc, the extended objects amount to about 40% of this total, and the scale has been chosen so that the line may thus indicate how the numbers of extended radio galaxies may be expected to continue beyond this distance. The filled circles show the numbers of cosmic rays apparently associated with the radio galaxies in each 20 Mpc — within 6° as in section 5. (The “error bars” show the effect of changing the source attribution from NGC 5090 to Cen A in 3 cases.) All these radio galaxies with jets have been included in these counts of associations, but only the extended (mostly FRI) radio galaxies mentioned by Nagar and Matulich showed an association. Thus the cosmic rays may indeed all originate within about 120 Mpc, though some sources may have been missed if the catalogue of Liu and Zhang is incomplete in the range 120-160 Mpc. The source peak near 50 Mpc is notable.

Hence, this treatment roughly confirms the z_{max} figure from the Auger optimization: it is probably below 120 Mpc for the set of particles that still have energies above 57 EeV when they arrive. This must be controlled by their maximum energy on production, and the rate at which they lose energy.

8. Implications of very local sources: a cut-off in the source spectrum?

If one receives few or no particles above E_{thresh} which originated beyond 100 Mpc, the energy of the particles released from the source must not be too high, and the rate of loss of energy, primarily through interactions with the cosmic microwave background radiation (CMBR), must be rapid, so that the energy falls below E_{thresh} within 100 Mpc. The rate of energy loss in the CMBR varies rapidly with proton energy, and it seems that the loss would be sufficient to drop below “57 EeV” within this distance only if, firstly, the particle energies are higher than quoted in the Auger paper, presumably because of remaining uncertainties in the fluorescence efficiency of air; and, secondly, the fall of the energy spectrum of cosmic rays must be steeper than that imposed by these energy losses: the observations must be closely approaching the upper energy limit of the accelerators.

There is as yet insufficient information to resolve the interplay of several relevant factors, but the general constraints will be described with the aid of Figure 12. Consider first the lines, which trace the average change in a proton’s energy with distance from its source. Ignoring the thicker lines, the steep dotted line, full line and dashed line refer to protons generated with energies of

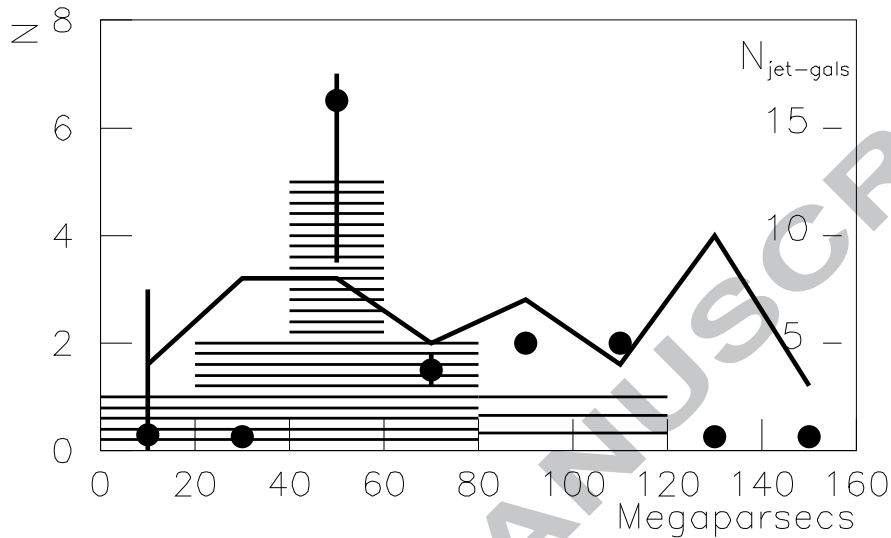


Figure 11: The histogram shows the numbers of extended radio galaxies as defined by Nagar and Matulich in 20 Mpc intervals. Beyond 75 Mpc the galaxies may have been chosen more selectively (see text). The line shows the number of galaxies with radio jets of at least 1 kpc [20] — in the field of view of the Auger Observatory, but without selection for lobe extension — the right hand scale applies to these. The black points are the numbers of cosmic rays that appear to be associated with these radio galaxies, none in fact being associated with non-extended galaxies. 3 cases attributed to NGC 5090 could alternatively be attributed to Cen A: the vertical lines show the changed counts that would result.

878 200 EeV, 100 EeV and 80 EeV respectively, and the horizontal axis shows the energies on arrival
 879 if they have travelled for the distances specified on the vertical axis since leaving the accelerator.
 880 (He nuclei are not considered as they photodisintegrate in ~ 1 Mpc, and larger nuclei are ignored
 881 because, apart from the magnetic deflection argument given in section 6, their mean path length
 882 for serious mass loss by photodisintegration is much less than 100 Mpc.) One expects to have a
 883 mixture of energies leaving the accelerator, with a larger number starting at the lower energies.
 884 It is seen that the expected distance distribution extends far above 100 Mpc, in contrast with the
 885 observations.

886 The only way to remove this tail of distant sources appears to be to assume that the reported
 887 energies are too low by a factor around 1.25, so that the true threshold energy is near 70 EeV.
 888 This makes the energy losses arising from photopion production reactions become much more
 889 rapid. The thicker dotted, full and dashed lines again refer to the proton energies after travelling
 890 various distances from the source, but assuming that the actual energies are always 1.25 times
 891 the figures written on the graph. The shaded area is roughly where we should expect to see the
 892 detected particles, on this basis, if there are few sources within 30 Mpc (as seems to be indicated
 893 by the data) and the source spectrum terminates not far from 100 EeV nominal energy (or 125
 894 EeV on a “corrected” energy scale): there would now be few particles having travelled more than
 895 100 Mpc. This is closer to the observed distance distribution.

896 However, if we attempt to estimate the distance from the source of individual particles, by

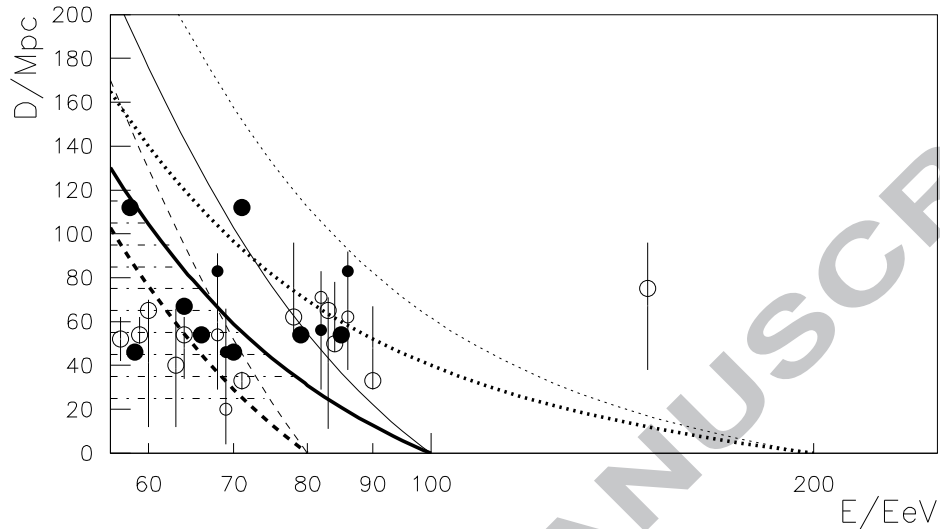


Figure 12: Distance of travel of particles arriving with different energies. For the observations, the distances are derived from redshifts of AGNs or radio-galaxies close to the line of sight (see text). The curves refer to the expected energy of protons generated with particular initial energies of 200, 100 or 80 EeV after they have travelled through the background radiation for different distances: thin lines for energies actually assigned in the Auger analysis, thick lines apply if the assigned (and plotted) energies are too low by a factor 1.25. The shaded area draws attention to the main area in which the points would be expected to lie in this latter case, assuming also that the source spectrum terminates near 100 EeV (“assigned energy”)

897 linking them to the AGNs seen close to the cosmic ray arrival direction, there is a problem. In
 898 outline, one expects that the particles arriving with the highest energies must have travelled a
 899 short distance, whilst the particles of lowest energy could come from a wide range of distances,
 900 with different starting energies. The observed data are presented as follows. The cosmic rays
 901 fairly clearly associated with extended radio galaxies (ERG) have a clear source distance, and
 902 are marked with large filled circles. For those not associated with extended radio galaxies, an
 903 open circle marks the median distance of VCV AGNs within 6° and a vertical line shows the
 904 range of distances amongst this group of possible source AGNs. Where there is an adjacent
 905 extended radio galaxy and several VCV AGNs, the ERG distance and the VCV median distance
 906 are both shown, using smaller symbols (unless the ERG distance agrees with the VCV median,
 907 when the VCV indications are ignored). (There is no nearby known AGN for one of the 21
 908 cosmic rays.) The expected correlation between energy and distance of travel is not apparent.
 909 The shape of the observed energy distribution is also a poor match, which might very possibly
 910 arise if there are event-to-event fluctuations in energy reconstruction accuracy of order 20% or
 911 more, which largely scramble the energies in such a small span of energies as is represented here
 912 — and reminiscent of the Haverah Park example discussed in section 4. A larger data sample
 913 is needed to make more of this energy spectrum, to find out just how steeply it must fall at this
 914 apparent termination. Simulations of energy propagation have been made but will be published
 915 separately.

916 **9. Summary: conclusions concerning the cosmic-ray sources**

917 The report [1] by the Auger collaboration, that most of the cosmic rays that had been detected
918 above an energy of 57 EeV came from directions within 3.2° of an optically detected AGN within
919 about 75 Mpc, listed in the 12th catalogue of Véron-Cetty and Véron, marked the first instance
920 of a fine-scale anisotropy clearly seen in charged-particle astronomy. It was shown in section 2
921 that cosmic rays appeared to come from regions where AGNs were clustered. Sky distributions
922 on different scales are consistent with the cosmic rays originating from sources in or near such
923 AGNs, typically Seyfert galaxies, and being deflected randomly by $3 - 4^\circ$ on their way to us. As
924 this scattering angle is similar to the separation of AGNs in the source region, it will not usually
925 be clear what object is the actual source. The appearance of some very weak objects closest to
926 the observed direction is hence not a problem. In section 3, a uniform-exposure polar plot was
927 recommended for displaying quantitative aspects of the distribution of cosmic rays and possible
928 source objects such as AGNs on the sky, and the distribution of cosmic rays was seen to follow
929 the distribution of the VCV AGNs on the large scale, with about 0.1 cosmic rays detected during
930 the reported observing run per catalogued AGN within 75 Mpc, where the exposure efficiency
931 was high.

932 A method of showing the close correlation with directions of AGNs or other objects that
933 did not require choice of a particular correlation “window” size was introduced in section 4
934 — a “right ascension resonance” in average closest distance — which showed the rapidity of
935 decoherence of these patterns on the sky when they were displaced slightly. This showed the
936 cross-correlation in a very immediate way, that could be used to explore related associations in
937 other regions. As this did not make use of any specially optimized window radius, it could be
938 used to check the very high statistical significance of the correlation with AGNs. The association
939 of cosmic rays with the extended radio galaxies with radio jets within 120 Mpc (Nagar and Mat-
940 ulich [3]), most of which were not in the VCV optically-based catalogue, was, quite separately,
941 significant at around the 1 in 10^6 level, with an average of around 1 detected cosmic ray per ob-
942 ject, although not all seem to be active at the present time: the nearby and spectacular low-energy
943 electron accelerators Cen A and Fornax A are probably currently switched off at these ultra high
944 energies (otherwise the former would have completely outshone the other FRI radio galaxies,
945 because of its proximity, as it does in the case of low-energy synchrotron radiation).

946 If the few brightest radio galaxies within ~ 80 Mpc, notably M87 (Virgo A), Cen A and
947 Fornax A, had been the dominant sources, their output must have been spread widely over the
948 sky by magnetic deflections [4, 5, 6]. However, only a small proportion of such widely-scattered
949 cosmic rays would line up within 3.2° of a catalogued AGN, as pointed out in section 3: this is
950 not the case. If, on the other hand, the lines-of-sight to cosmic ray sources are scattered around
951 many VCV AGNs by $3 - 4^\circ$, most of the cosmic ray distributions are well described. In summary,
952 the small apparent scale of $3 - 4^\circ$ for the spread of cosmic ray directions around source regions
953 indicates that there are many more sources than there are strong radio-emitting AGNs. So al-
954 though perhaps 40% of the detected cosmic rays in this energy region appear to come from FRI
955 or similar radio galaxies at typical distances near 50 Mpc, the remainder presumably come from
956 numerous weaker sources, which reside in these AGN clusters, and accelerate protons to very
957 similar maximum energies. Ghisellini et al [12] have also emphasised the possibility that any
958 objects that reside in galaxy clusters are candidates, and have shown that cosmic-ray directions
959 correlate with the density of ordinary galaxies. It is not known whether the pattern de-coheres
960 with galaxy density as rapidly as with AGNs, but it seems likely that AGNs do trace galaxy den-
961 sity. Although these authors particularly draw attention to the possibility that magnetars might

962 be the sources [22], the very significant appearance of FRI radio galaxies close to the directions
 963 from which cosmic rays arrive makes it appear likely that the Seyfert galaxies are indeed the cur-
 964 rently less-active end of a distribution of jet-related sources of cosmic rays of $(0.7 - 1.2) \times 10^{20}$ eV.
 965 (Only 25% of the VCV AGNs are not known radio emitters.) A separate population of numerous
 966 low-fluence non-AGN sources may yet make a contribution, though. As it is apparently the case
 967 that the particles, which, it is argued, are largely protons at the very highest energies, can rarely
 968 reach us from more than 100 Mpc away, it appears that the true energies must be around 25%
 969 higher than currently estimated by the Auger methods, and that the accelerator output probably
 970 drops rather sharply in the region of 1.2×10^{20} eV. It is, however, surprising that this assembly of
 971 stronger and weaker sources produces a total spectrum with a sharp cut-off.

972
 973 *Postscript* Although further Auger observations have not yet been published, talks (e.g. [23])
 974 indicate that a later exposure has given a very different sky distribution, without the same con-
 975 centration near AGNs. As was shown above, the published data show correlations with AGNs
 976 and related objects that are not accidental; but the success of a 57 EeV threshold, for example, in
 977 extracting the vital proton component that can point back to sources may not be robust, as seen
 978 in the comparison of sky maps from three experiments at the end of section 4. The success of the
 979 initial phase might even, for instance, have depended on the presence of excessive fluctuations
 980 in (proton) energy reconstruction (in the context of a very steeply falling spectrum), occurring
 981 in somewhat smaller fields of less well-behaved detectors, that falsely promoted the energies
 982 of some protons! It seems that the recognition of proton-induced showers will be an important
 983 task. The appearance of very widely-scattered cosmic ray directions near the maximum ener-
 984 gies gives support to the indication from the Auger studies on depth of shower maximum [19]
 985 that a heavy-nucleus component becomes very important as the extreme energies are approached.

986 *Acknowledgements*

987
 988
 989 I wish to thank Ralph Engel for stimulating me to offer suggestions on the Auger directions,
 990 both Alan Watson and Johannes Knapp for several critical and perceptive discussions and much
 991 encouragement, information and help, Jeremy Lloyd Evans and Jim Hinton for useful sugges-
 992 tions, and Mansukh Patel and Ronald Bruijn for further help.

993 **References**

- 994 [1] The Pierre Auger Collaboration: J. Abraham et al., (2008) *Astroparticle Physics* 29: 188-204; and
 995 (2007) arXiv (astro-ph) 0712.2843 v1.
 996 [2] M-P Véron-Cetty and P Véron: *Astron. Astrophys.* 455 (2006) 773:
 997 accessed via <http://vizier.u.strasbg.fr/viz-bin/VizieR> .
 998 [3] N M Nagar and Matulich J (2008) *subm. Astron. Astrophys.*; and arXiv:0806.3220v1 [astro-ph].
 999 [4] P L Biermann et al. (2008), arXiv:0811.1848v3 [astro-ph]
 1000 [5] P L Biermann (2008), lectures at 400th Heraeus Seminar
 1001 <http://www-ik.fzk.de/ik/Heraeus400/talks/15-Biermann.pdf>
 1002 [6] D S Gorbunov, Tinyakov P G, Tkachev I I and Troitsky S V (2008): arXiv:0804.1088v1 [astro-ph].
 1003 [7] M R George, Fabian A C, Baumgartner W H Mushotzky R F and Tueller J (2008), *MNRAS* . arXiv:0805.2053v1
 1004 [astro-ph].
 1005 [8] I V Moskalenko, Stawarz I, Porter T A and Cheung C C (2008) *subm. Astrophys. J.*, and arXiv:0805.1260v1
 1006 [astro-ph]
 1007 [9] T Stanev (2008) lecture at 400th Heraeus Seminar
 1008 <http://www-ik.fzk.de/ik/Heraeus400/talks/07-Stanev-Intro.pdf>
 1009 [10] R U Abassi et al.: The High Resolution Fly’s Eye Collaboration (2008) *Astroparticle Physics* 30: 175-9.

- 1010 [11] Ingyin Zaw, Farrar Glennys R and Greene Jenny E (2008): arXiv:0806.3470v1 [astro-ph]
 1011 [12] G Ghisellini, Ghirlanda G, Tavecchio F, Fraternali F and Pareschi G (2008): MNRAS ; arXiv:0806.2393v1 [astro-
 1012 ph].
 1013 [13] G Cunningham et al. (1980) Ap.J. Letters 236: L71
 1014 [14] The Pierre Auger Collaboration (2007) Science 318: 938-43.
 1015 [15] web-site http://physics.rutgers.edu/~lsct/agn/high_e_events.txt
 1016 [16] S Westerhoff et al. Nucl. Phys. B (Proc. Suppl.) 136 (2004) 46-51
 1017 [17] M Ave, Hinton J A, Knapp J, Lloyd-Evans J, Marchesini M and Watson A A (2001) 27th Int. Cosmic Ray Conf.,
 1018 Hamburg (Copernicus Gesellschaft) 1: 381.
 1019 [18] Y Uchihori et al. (1996), Extremely High Energy Cosmic Rays: Astrophysics and Future Observatories (ed. M
 1020 Nagano, U. of Tokyo): 50.
 1021 [19] M Unger for the Pierre Auger Collaboration (2007), 30th International Cosmic Ray Conference, Merida, Vol 4 (HE
 1022 part 1) p 373
 1023 [20] F K Liu and Zhang Y H (2002) Astron. Astrophys. 381: 757-60.
 1024 List only available electronically: <http://cdsweb.u-strasbg.fr/cgi-bin/qcat?J/A+A/381/757>
 1025 [21] A M Hillas (1984) Ann. Revs. Astron. Astrophys. 22: 425
 1026 [22] J Arons (2003) Astrophys. J. 589: 871
 1027 [23] S Westerhoff (2009) APS 2009 March: http://blogs.nature.com/news/blog/2009/05/aps_2009_pierre_auger_backs_of.html

1028 A. AGN counts in Véron-Cetty Véron 12th edition catalogue

1029 Figure 13 shows the number of objects listed in the southern hemisphere (declination $< +34^\circ$)
 1030 per Mpc of distance, D , converting from redshift to distance using a value $H_o = 72 \text{ km s}^{-1} \text{ Mpc}^{-1}$
 1031 for Hubble's constant. The lines refer to objects in different ranges of absolute magnitude (" -19 "
 1032 indicating -19.0 to -19.9 , for example).

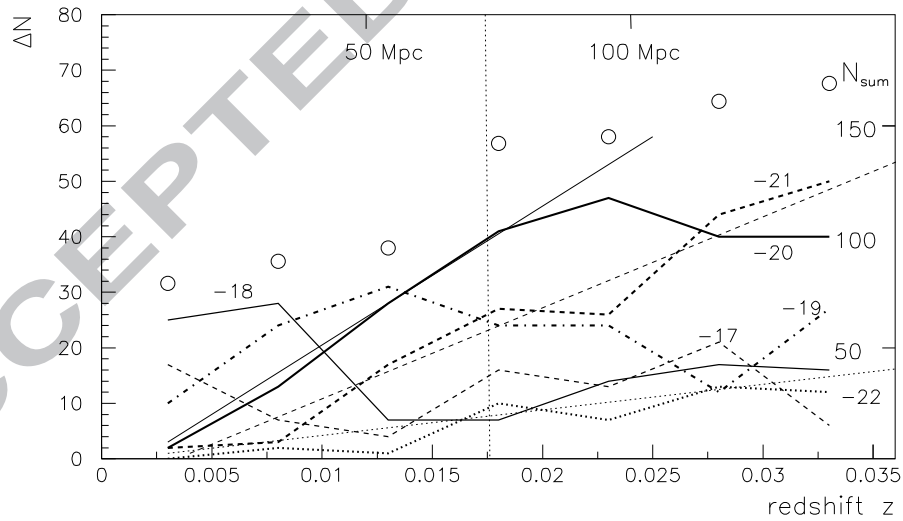


Figure 13: Distribution in distance of AGNs (declination $< +34^\circ$) in VCV catalogue. Lines marked -17 ... -21 refer to AGNs having absolute magnitude -17.0 to -17.9 , -18.0 to -18.9 , -21.0 to -21.9 . Line -22 refers to all magnitudes brighter than -22.0 (though only 27% of those included are brighter than -22.9). For the three brighter groups, a dotted line shows the straight-line trend. Open circles show totals (scale on right).

1033 The lines -20, -21 and -22 suggest a trend $dn/dD \propto D$ initially, as though the objects are
 1034 distributed in a slab whose thickness is a few Mpc, but then falling sharply below this trend as
 1035 though there is a limiting apparent magnitude for efficient detection. Thus objects with absolute
 1036 magnitude brighter than -20.0 would be recorded inefficiently at distances beyond the 75 Mpc
 1037 limit of the Auger sample. The median absolute magnitude for the most closely associated AGNs
 1038 at the closer distances appears to be about -19.0, so beyond 75 Mpc, the catalogue would fail to
 1039 list many of any truly associated AGNs (as remarked in [1], and one would need large statistics
 1040 to map out the sources beyond there. If the number of listed AGNs within 75 Mpc had been
 1041 much greater, the probability of associations within 3.2° with any arbitrary direction would have
 1042 been large, nullifying the signal.

1043 B. Array exposure to different celestial directions: equal-exposure plot radius.

The effective detection area presented to a source at zenith angle θ is $A \cdot \cos \theta$ if the detecting
 area on the ground always has a fixed value A . Let λ be the magnitude of the observatory's
 latitude (i.e. always treated as positive). For a source at polar angle p , its zenith angle varies
 during the sidereal day according to the expression

$$\cos \theta = \cos p \cdot \sin \lambda + \sin p \cdot \cos \lambda \cdot \cos H \quad (2)$$

where H is the hour angle relative to the source's right ascension, which increases uniformly with
 time, from 0 when θ is least (source highest in the sky), to 360° after a complete sidereal day.
 Thus the time average of the effective detecting area is

$$\langle A \cdot \cos \theta \rangle = A \int \cos \theta \cdot dH/360^\circ \quad (3)$$

1044 where the integral is taken over all values of H (here expressed in degrees) which give $\theta < \theta_{max}$
 1045 . For the Auger array, $\theta_{max} = 60^\circ$ and $\lambda = 35.2^\circ$. At polar angles greater than $(90^\circ + \theta_{max} - \lambda)$
 1046 sources never rise to zenith angles less than θ_{max} : this limit is 114.8° for the Auger observatory,
 1047 meaning that sources with declinations above $+24.8^\circ$ are never recorded. Where $\theta_{max} > 90^\circ - \lambda$,
 1048 as at Auger, some ("circumpolar") sources never fall further from the zenith than θ_{max} : they have
 1049 $p < \theta_{max} - (90^\circ - \lambda)$ and are detectable all day. If $\theta_{max} \leq 90^\circ - \lambda$, though, sources closer to the
 1050 pole than $p' = 90^\circ - \theta_{max} - \lambda$ are never recorded (and on an equal-exposure plot, this range $0..p'$
 1051 is contracted to a point at the centre of the plot). To find the effective detecting area for a source
 1052 at any selected polar angle p , the integral in equation 3 is evaluated over the range of H for which
 1053 θ is less than θ_{max} , noting that for some values of p this condition is always or never satisfied, as
 1054 just mentioned.

Having determined the efficiency of the detector for sources of each polar angle, as just
 described, the radius R at which a source should be shown in an equal-exposure plot is

$$R(p) = k \sqrt{\int_{z=0}^{z=p} \langle A \cos \theta \rangle \sin z \cdot dz}, \quad (4)$$

1055 where the variable z refers to a polar angle, and $\langle A \cos \theta \rangle$ is a function of this polar angle, from
 1056 equations 3 and 2. The limit of integration, p , is the polar angle at which R is required. k
 1057 is chosen to make $R \rightarrow 1$ at large p . Table 4 tabulates the calculated efficiency and polar-
 1058 plot radius, R , at intervals of 2° in polar angle. The numerical results can be represented to a
 1059 reasonable approximation by the following formula:

For the Pierre Auger Observatory,

$$R = [1 + 0.27 \exp(-p/5.7^\circ)] \cdot \sin(0.746p), \quad (p \text{ in degrees}) \quad (5)$$

1060 with the maximum divergence from the tabulated value being 0.006. However, if the term in
 1061 square brackets is removed, leaving just the sine, the error is only significantly increased at polar
 1062 angles $< 16^\circ$, reaching 0.012 at 8° , and as few cosmic rays are detected so close to the pole, this
 1063 small distortion in their plotted density is probably immaterial. This formula should not be used
 1064 for polar angles beyond the theoretical maximum of 114.8° .

1065 To plot a cosmic-ray direction, or an astronomical object, at right ascension α and declination
 1066 δ , the polar distance is calculated ($p = 90^\circ - \delta$ for a northern hemisphere plot, or $p = 90^\circ + \delta$ for
 1067 the southern hemisphere), then R is found by interpolation in the table or by use of approximation
 1068 given in equation (5). The coordinates on the plot are then $x = R \cdot \cos \alpha$, $y = R \cdot \sin \alpha$.

p	Efficiency	R	p	Efficiency	R
0	0.576	0.000	60	0.331	0.702
2	0.576	0.030	62	0.325	0.720
4	0.575	0.061	64	0.319	0.739
6	0.489	0.090	66	0.312	0.756
8	0.436	0.115	68	0.305	0.774
10	0.413	0.140	70	0.298	0.791
12	0.401	0.163	72	0.290	0.807
14	0.394	0.187	74	0.282	0.822
16	0.389	0.211	76	0.274	0.837
18	0.387	0.234	78	0.265	0.852
20	0.385	0.258	80	0.256	0.866
22	0.383	0.282	82	0.246	0.879
24	0.382	0.306	84	0.237	0.892
26	0.381	0.329	86	0.227	0.904
28	0.380	0.353	88	0.216	0.915
30	0.379	0.376	90	0.206	0.926
32	0.378	0.400	92	0.195	0.936
34	0.377	0.423	94	0.183	0.945
36	0.375	0.446	96	0.172	0.954
38	0.373	0.469	98	0.160	0.962
40	0.371	0.492	100	0.147	0.969
42	0.369	0.514	102	0.135	0.976
44	0.366	0.536	104	0.121	0.981
46	0.363	0.558	106	0.107	0.987
48	0.359	0.580	108	0.092	0.991
50	0.356	0.601	110	0.075	0.995
52	0.351	0.622	112	0.056	0.998
54	0.347	0.643	114	0.029	1.000
56	0.342	0.663	116	0.000	1.000
58	0.337	0.682			

Table 4: Detection efficiency and radial position R in equal-exposure polar plot for the Auger Observatory.